THESIS APPROVAL

The abstract and thesis of Amy Francis Ebnet for the Master of Science in Geology were presented October 31, 2005, and accepted by the thesis committee and the department.

COMMITTEE APPROVALS:

_____
Andrew G. Fountain, Chair

_____
Christina L. Hulbe

_____
Scott F. Burns

_____
Roy W. Koch
Representative of the Office of Graduate Studies

DEPARTMENT APPROVAL:

_____
Michael L. Cummings, Chair
Department of Geology

ABSTRACT

An abstract of the thesis of Amy Francis Ebnet for the Master of Science in Geology presented October 31, 2005.

Title: A Temperature-Index Model of Stream Flow in Taylor Valley, Antarctica.

The McMurdo Dry Valleys of Antarctica are a polar desert with alpine glaciers, ephemeral streams, and perennially ice-covered lakes. Essentially all water in the lakes and streams originates as glacier melt during the austral summer. Because summer temperatures hover near the melting point, small variations in the energy balance cause the melt water flux to vary from season to season by as much as an order of magnitude. I developed a model for stream flow volume in Taylor Valley, one of the dry valleys, for the purpose of estimating flow over decades to millennia. Three simple statistical models were developed using measured stream discharge and glacier ablation, a model based solely on air temperature, one including the additional

variable spatial variations in solar radiation and one including the additional variable summer average wind-speed. Results showed that melt-water flow increased exponentially as summer average air temperatures warmed to 0°C. A temperature-based model was sufficient to predict stream flow volume from the north-facing or south-facing glaciers but not the two together. The inclusion of spatial variations in solar radiation allowed both north and south facing glaciers to be modeled. In the Fryxell and Hoare basins, model results showed r^2 values of 0.60 and 0.67 respectively from the temperature-based model and 0.73 and 0.42 from the model including solar radiation. Modeling results for the Bonney Basin were poor partly due to large differences in energy balance controls on the glaciers. Glaciers in the Bonney Basin are characterized by steep slopes and rough surfaces which are important contributors towards melt and are not accounted for in the models. The third model attempted to account for the variation in wind speed throughout the valley with little improvement. The models predict melt at summer average temperatures below 0°C with threshold temperatures ranging from -4.9°C to -5.5°C.

A TEMPERATURE-INDEX MODEL OF STREAM FLOW IN TAYLOR VALLEY, ANTARCTICA

by

AMY FRANCIS EBNET

A thesis submitted in partial fulfillment of the
requirements for the degree of

MASTER OF SCIENCE
in
GEOLOGY

Portland State University
2005

ACKNOWLEDGEMENTS

I would like to thank Andrew G. Fountain for giving me the opportunity to do this research and the guidance to see it through. I also was to thank Thomas Nylen for his advice and help with fieldwork, my fellow graduate students for making graduate school fun and interesting and my husband, Jon and my parents, Ken and Harriet for their love and support. Funding for this work came from NSF OPP 0096250.

TABLE OF CONTENTS

LIST OF TABLES

LIST OF FIGURES

I INTRODUCTION

The McMurdo Dry Valleys (MDV) of Antarctica are a polar desert with alpine glaciers, ephemeral streams, and perennially ice-covered lakes. The ecosystem consists of microorganisms, mosses, lichens and a few invertebrates which inhabit the streams, lakes and soils of the MDV. The region receives little precipitation (snow) and essentially all water in the streams and lakes originates as glacier melt (Fountain and others, 1999a). Because summer temperatures hover near and often below the melting temperature, small variations in the available energy for melt cause the seasonal melt-water flux to vary by as much as an order of magnitude. Consequently, the ecosystem in the MDV is extremely sensitive to small changes in the energy balance of the glaciers. The study of melt-water production from the glaciers is therefore important for understanding the controls on the structure and function of the ecosystem. Melt-water production in response to climate change is also important for understanding the paleo-hydrology of the MDV.

The purpose of this thesis is to develop a simple model of glacial melt-water production to the lakes in Taylor Valley, one of the MDV, for the eventual purpose of estimating the paleo-hydrology over millennia. This work will aid our understanding of long-term hydrologic changes and contribute to understanding the ecosystem response.

Climate and Setting

The MDV are located on the west coast of McMurdo Sound at 77°00'S 162°52'E (Figure 1). They cover an area of approximately 4800 km^2, the largest

relatively ice-free area in Antarctica (Fountain and others, 1999a). The MDV are relatively ice-free because the Transantarctic Mountains block much of the ice-flow off the east Antarctic Ice Sheet toward McMurdo Sound (Chinn, 1990). Taylor Valley, approximately 36 km long, with an area of about 400 km^2 (Lewis and others, 1999), is bounded by the Asgard Range to the north and the Kukri Hills to the south.

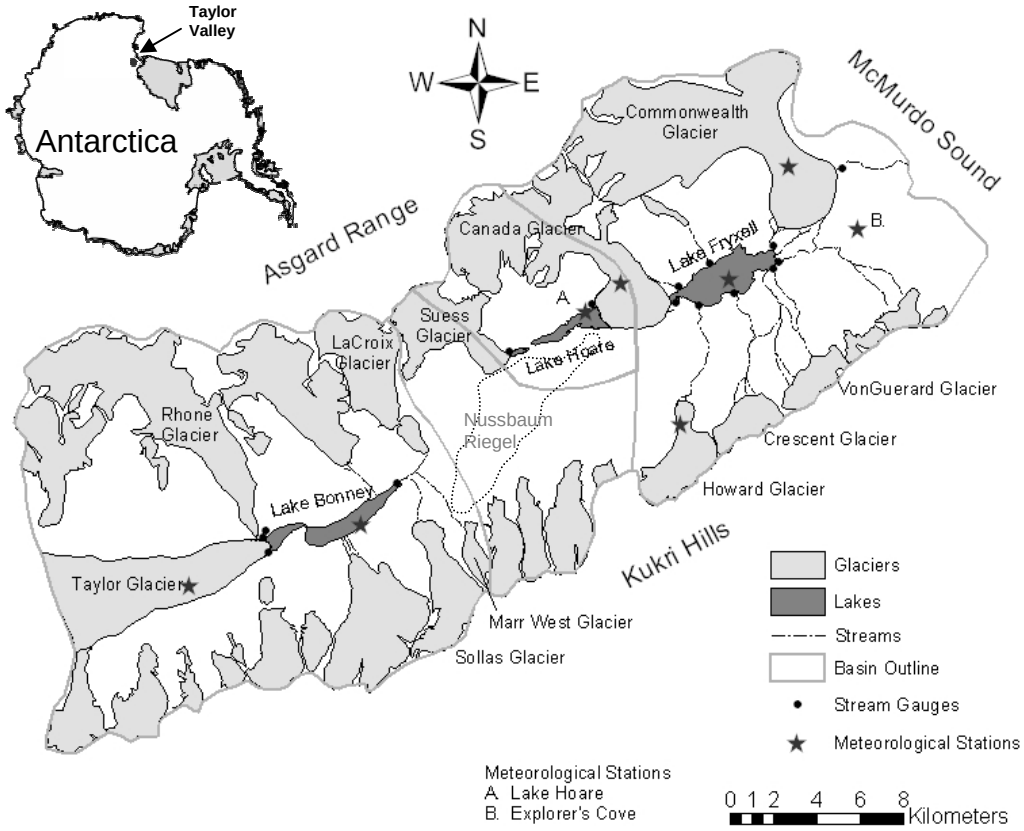

Figure 1: Site map of Taylor Valley, Antarctica showing locations of glaciers, lakes, stream gauges and meteorological stations.

Taylor Valley contains about 26 alpine glaciers flowing from the adjacent mountain ranges and more than 24 ephemeral streams (Fountain and others, 1999a) that drain melt-water from the glaciers into three large perennially ice-covered lakes (Bonney, Hoare and Fryxell) located on the valley bottom. The mean annual

precipitation in the valley bottom is less than 10 cm water equivalent (weq) (Fountain and others, 1999a) making the valley a polar desert. Mean annual temperature varies between –14.8 and –23.0°C (Doran and others, 2002) with mean summer temperatures of about -2°C. Monthly average wind speeds range from 2-4 m s^{-1} and tend to increase from the coast inland (Nylen and others, 2004; Doran and others, 2002; Fountain and others, 1999a). Katabatic winds flow off the ice sheet and warm adiabatically as they descend into the valley creating a warmer and drier atmosphere (Nylen and others, 2004; Doran and others, 2002). This favors sublimation and limits the energy available for melt. An up-valley (away from the coast) gradient in climate exists with increasing air temperatures, decreasing humidity, decreasing precipitation, and higher wind speeds (Doran and others, 2002; Fountain and others 1999b). The climatic differences along the valley are enhanced by the Nussbaum Riegel, a 700 m high hill that bisects the valley 20 km from the coast between the Hoare and Bonney basins (Fountain and others, 1999b).

Glacial melt streams flow to the ice-covered lakes for 4 to 10 weeks during the austral summer (McKnight and others, 1999). Some water is lost from the streams directly through evaporation to the atmosphere or indirectly through the hyporheic zone (Bomblies, 1998). None of the three lakes have an outlet and are surrounded by permafrost so the only loss of volume from the lakes is through sublimation of the ice cover or evaporation from the surface water (Bomblies, 1998).

Taylor Valley glaciers flow from the Asgard Range and the Kukri Hills. Taylor Glacier, an outlet glacier of the East Antarctic Ice Sheet, flows into the valley from the

west (Figure 2). All of the larger glaciers (e.g. Taylor, Canada, and Commonwealth) terminate in vertical cliffs. The north-facing glaciers in the Kukri Hills have higher equilibrium line altitudes (ELA) than the south-facing glaciers in the Asgard Range due to differences in solar radiation (Fountain and others, 1999b). Because of topographic differences, the glaciers in the Asgard Range have larger accumulation basins making them larger than the glaciers in the Kukri Hills. Cool, dry, and windy conditions during summer favor sublimation over melt (Chinn, 1987) and account for 40% - 80% of the ablation on Canada Glacier (Lewis and others, 1998) and 56% ablation on Taylor in 1994-1995 (Johnston, 2004). Melt can occur at air temperatures below 0°C (Chinn, 1987; Lewis and others, 1998), some of which occurs in the subsurface through a solid-state greenhouse effect (Fountain and others, 2004). Differences in the energy balance allow cliff faces to melt while the upper surface of the glacier remains frozen (Chinn, 1987). Cliffs can contribute up to 20% of the total melt-water runoff (Lewis and others, 1998).

Figure 2: Taylor Glacier.

Melt Models

Surface melt on glaciers is determined by energy exchange to and from the glacier surface. Energy is primarily exchanged through net radiation *(R)*, sensible heat *(H)*, latent heat *(L)*, heat conduction through the ice *(G)* and melt *(M)*,

$$R + H + L + G + M = 0 \tag{1}$$

Each term of (1) (except *M*) can be determined from measurements of radiation, air and ice temperatures, wind speed and vapor pressure. Energy for melt is calculated as a residual from (1) (Paterson, 1994). Complete energy balance models require detailed meteorological measurements, which are difficult to collect and are typically unavailable for long periods of time. We wish to estimate melt for times that predate detailed meteorological measurements, so we adopt an alternative approach, a temperature-index model, in which melt is related to air temperature (T) alone. The simplest form of temperature-index model is,

$$M = FT \tag{2}$$

where F is a factor of proportionality and T is air temperature. Typically M and T are daily values. Another form is to use only temperatures above 0 °C (positive degree-day) to calculate daily melt,

$$\sum_{i=1}^{n} M = F \sum_{i=1}^{n} T^{+} \cdot \Delta t \tag{3}$$

The summation on the right-hand side of equation (3) is the sum of positive air temperatures over a day where T^{+} is a temperature >0°C measured over a time interval

Δt (Hock, 2003). The factor F in both equations varies according to the relative importance of terms in (1) (Braithwaite, 1995; Hock, 2003). For example, F is greater for low albedo snow/ice and high elevation because increased net solar radiation produces more energy for melt. F is smaller in conditions of high sublimation because sublimation reduces the energy available for melt. To estimate melt for conditions colder than 0°C, which occur in the MDV, a melt threshold temperature can be defined,

$$M = \begin{cases} F(T_d - T_0) : T_d > T_0 \\ 0 : T_d \leq T_0 \end{cases} \tag{4}$$

where T_0 is a threshold temperature below 0°C and F is a factor of proportionality (Hock, 2003).

Temperature-index models generally perform well despite their great simplicity because air temperature is a factor in all terms in the energy balance equation, except for shortwave radiation (Braithwaite, 1981; Ohmura, 2001). Although net radiation is usually the largest heat source to the surface (Braithwaite, 1981; Ohmura, 2001), it does not correlate particularly well with melt because unlike temperature, daily and monthly net radiation are not as variable as melt (Braithwaite, 1981). Temperature-index models are widely used because air temperature data are widely available and easy to interpolate and forecast (Hock, 2003). However, they fail to account for spatial variations in melt due to spatial changes in the energy balance (Hock, 1999). The accuracy of index models also decreases with shorter time intervals because they ignore the temporal changes in the energy terms, which may

overwhelm the effects of temperature (Hock, 2003). Attempts to improve melt predictions usually involve temporal changes in some of these terms (e.g. Hock, 1999; Kane and Greck, 1997; Kustas and Rango, 1994).

Previous works on melt-water modeling in the MDV have used both energy balance (Chinn, 1987; Lewis and others, 1998; Lewis and others, 1999) and temperature-index models (Dana and others, 2002; Jaros, 2003). The model of Dana and others (2002) used advanced very high resolution radiometer (AVHRR) satellite brightness temperatures of the dry valleys to estimate diurnal and seasonal discharge. Using 1.1 km resolution pixels, they found a good correlation between the number of pixels with temperature greater than -14°C and discharge. Given the frequent AVHRR coverage of the valley, Dana and others (2002) were able to predict flow biweekly. Jaros (2003) modeled the spatial variations in melt water production based on the temperature lapse rate but not the seasonal variation. Bomblies (1998) examined spatial variations of stream flow based on patterns of solar shading on the glaciers.

Here, I build the work of Jaros (2003) and Bomblies (1998) and model both spatial and temporal variations in melt water production to estimate stream flow volume. I present three simple models to predict total summer (December-January) melt-water runoff from all of the glaciers contributing to the three major lakes in Taylor Valley. In addition to a basic temperature-index model, I examine a temperature and solar-radiation index model, and a model that includes wind speed. The models calculate specific melt (m^3m^{-2} water equivalent) over the glacier surface, and stream flow volume is estimated by the product of melt and surface area of the

glacier. Independent field measurements of glacier mass balance are used to constrain the magnitude of the estimated melt while measured stream flow is used to constrain the estimated stream flow volume.

II DATA AND PRELIMINARY ANALYSIS

Streams

Stream flow measurements in the MDV are important to the monitoring of lake level change because the streams are the only major source of water to the lakes (McKnight and others, 1994). Stream flow is also important for nutrient budgets in the lakes, a critical factor for lake ecosystems (McKnight and others, 1994). Measurements of stream flow began in Taylor Valley in the 1990-1991 summer season and have continued to the present (except for the 1992-1993 season). Eight streams are monitored continuously in the Fryxell Basin, two in the Hoare Basin, four in the Bonney Basin, and one that flows to the coast (Figure 1). Stream stage is generally recorded at 15-minute intervals by a pressure sensor and converted to discharge (liters per second) via rating curves developed from discharge measurements (McKnight and others, 1994). Accurate stage measurements are difficult because of stream icing at low flow and the unstable nature of the stream channels during high flow (McKnight and others, 1994). The data quality is assessed during each visit to the measurement sites and a quality level of good, fair or poor is assigned to each measurement (Cozzetto, K., personal communication, 2004). Good stream flow measurements are considered accurate to within 10% whereas poor measurements may be inaccurate by more than 25% (http://huey.colorado.edu/, 2004).

Some stream-flow records are missing in the eleven-year period and were replaced by estimates based on flows from Canada Stream flowing from Canada Glacier. Canada Stream has the longest and most complete record of all monitored

streams in MDV. The monthly stream flow volume for Canada Stream correlates well with most of the streams in the valley (Jaros, 2003). Linear correlations of Canada Stream volume with eight other streams (Andersen, Green, Commonwealth, Lost Seal, Delta, House, Priscu, Lawson, Lyons, Santa Fe) were significant at the $1x10^{-9}$ level of significance (all p-values were less than $4x10^{-10}$) and r^2 values ranged from 0.77 to 0.97 (Figure 4). The data quality of Lyons and Santa Fe streams draining from Taylor Glacier (Bonney Basin), are poor with frequent data gaps. These streams are subject to unstable stream channels and large sediment loads (Jaros, C., personal communication, 2004). Consequently, no significant correlation between these two streams and Canada Stream exists with the available data (Figure 4). For the rest of the stations, only nineteen of 143 seasons of record were estimated for the thirteen streams (Table 1).

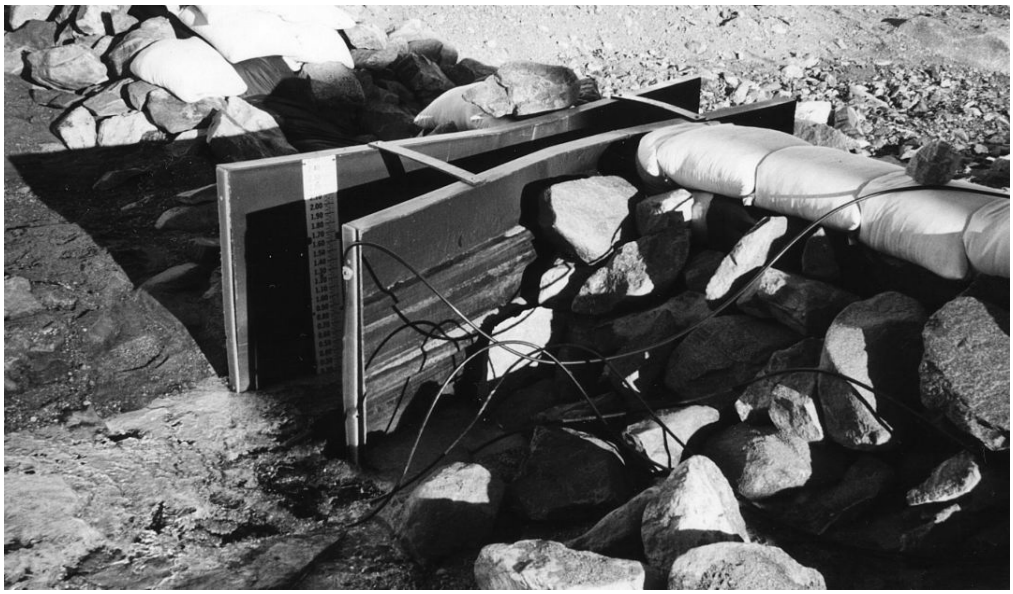

Figure 3: Stream gauge on Andersen Creek. Photo by Jonathan Ebnet, 2005.

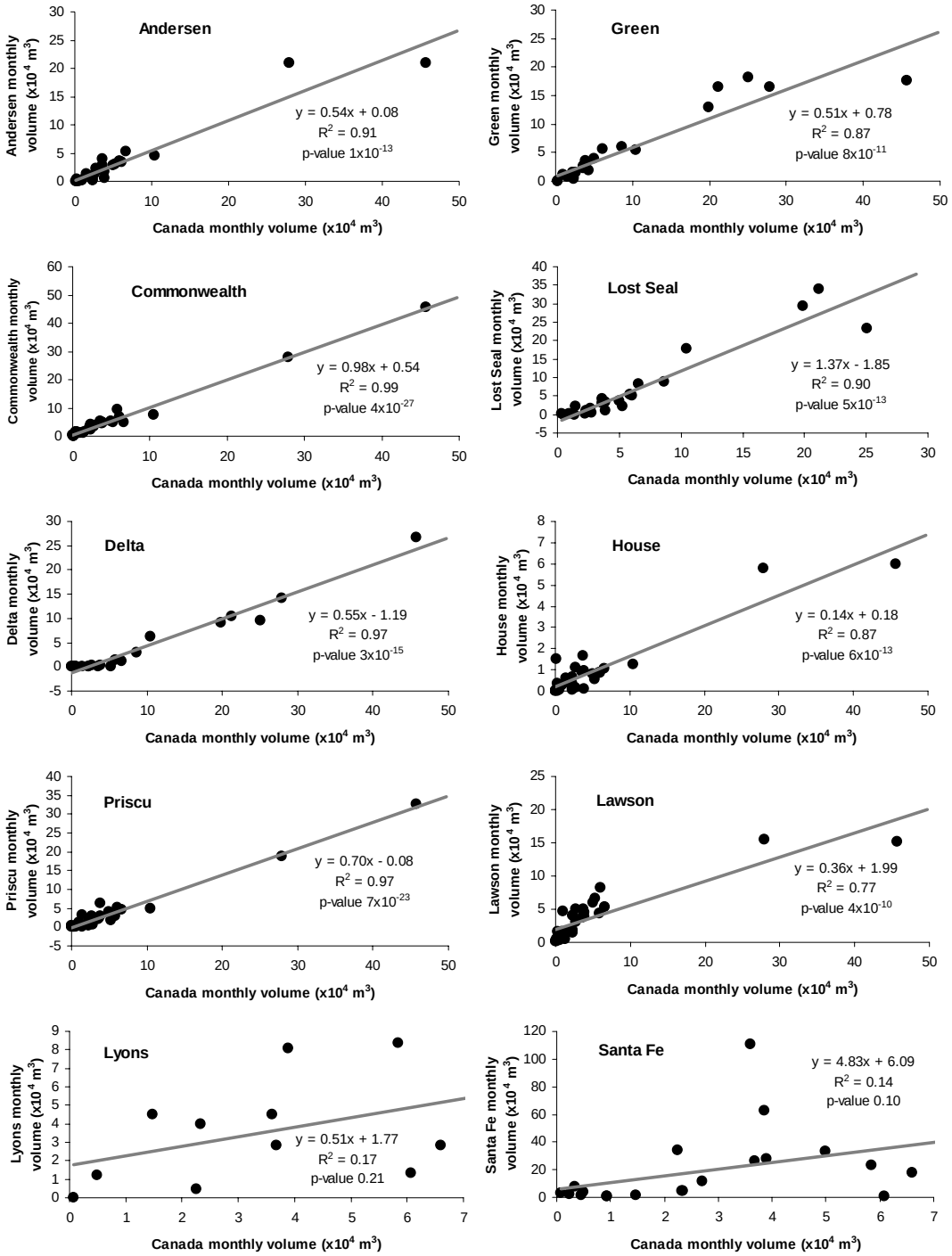

Figure 4: Linear regressions between Canada Stream and streams with incomplete flow records in Taylor Valley. Data obtained from http://huey.colorado.edu/, 2004.

Table 1: Total yearly stream flow volume (m^3). – indicates missing data and * indicates seasons where at least one month of data was estimated from Canada Stream. †The estimated stream flow volume for Huey Creek in 94-95 was negative. Original data obtained from http://huey.colorado.edu/.

Basin	Stream	90-91	91-92	93-94	94-95	95-96	96-97
Fryxell Basin	Canada	501,609	299,657	130,138	41,704	109,654	93,011
	Green	330,315	223,956	58,251	27,232	68,037	66,060
	Lost Seal	525,858	429,060	185,525	19,536	64,959	46,376
	Aiken	249,898	278,849	57,047	9,447	25,048	33,298
	Delta	186,860	135,312	63,312	2,468	*24,075	*25,387
	Crescent	208,009	80,447	38,569	1,920	7,651	7,844
	VonGuerard	159,018	140,807	67,708	5,864	6,527	4,593
	Huey	151,278	34,807	48,056	--†	*9,712	4,221
Hoare Basin	House	*71,629	*48,730	19,865	14,487	13,912	9,003
	Andersen	*268,856	*161,155	47,954	14,808	41,479	44,780
Bonney Basin	Lyons	--	--	--	--	53,478	--
	Santa Fe	--	--	--	118,687	97,278	978,154
	Lawson	*262,008	*168,649	*126,829	100,042	135,372	109,869
	Priscu	*318,090	*207,209	63,531	41,214	75,282	70,996
New Harbor	Commonwealth	*512,712	*309,561	114,917	61,622	134,610	115,031

Basin	Stream	97-98	98-99	99-00	00-01	01-02
Fryxell Basin	Canada	76,859	131,843	85,334	93,662	760,594
	Green	57,072	*79,091	48,331	*71,197	*360,019
	Lost Seal	57,517	138,099	73,019	27,646	*687,734
	Aiken	36,975	107,819	19,557	8,588	742,847
	Delta	6,120	25,665	767	69	407,255
	Crescent	5,380	10,236	180	0	158,737
	VonGuerard	720	7,248	0	0	275,987
	Huey	3,218	1,094	1,743	0	*221,856
Hoare Basin	House	30,750	19,508	31,747	7,069	117,980
	Andersen	25,729	88,550	73,027	*59,700	425,739
Bonney Basin	Lyons	130,544	124,010	73,340	--	--
	Santa Fe	657,477	470,223	1,458,988	--	--
	Lawson	76,221	114,311	119,107	102,406	324,791
	Priscu	111,992	78,083	46,344	25,255	518,172
New Harbor	Commonwealth	94,859	156,712	101,052	99,351	760,594

Meteorological Data

Eight meteorological stations collect data year-round in Taylor Valley (Figure 1). Four stations are located on glaciers – one each on Commonwealth, Canada, Taylor, and Howard glaciers. The other four stations are located on the valley floor – three on the shores of each of the lakes and one at Explorer's Cove near the coast. Each meteorological station (Figure 5) measures air temperature, relative humidity, wind speed and direction and incoming shortwave radiation (Doran and others, 2002). Some stations also measure outgoing shortwave radiation, incoming and outgoing longwave radiation, net radiation, ice/soil temperature, and ice ablation. Data sampling intervals over the period of record ranged from 30 to 60 seconds, and averaging intervals ranged from 10 minutes to 6 hours (Doran and others, 2002). The averaging interval was set to 15 minutes for all stations starting in November 1995. The meteorological station at Lake Hoare, starting in December of 1985, contains the longest record (Clow and others, 1988). Most of the other stations were installed in 1993-1994 with a few added in the following years.

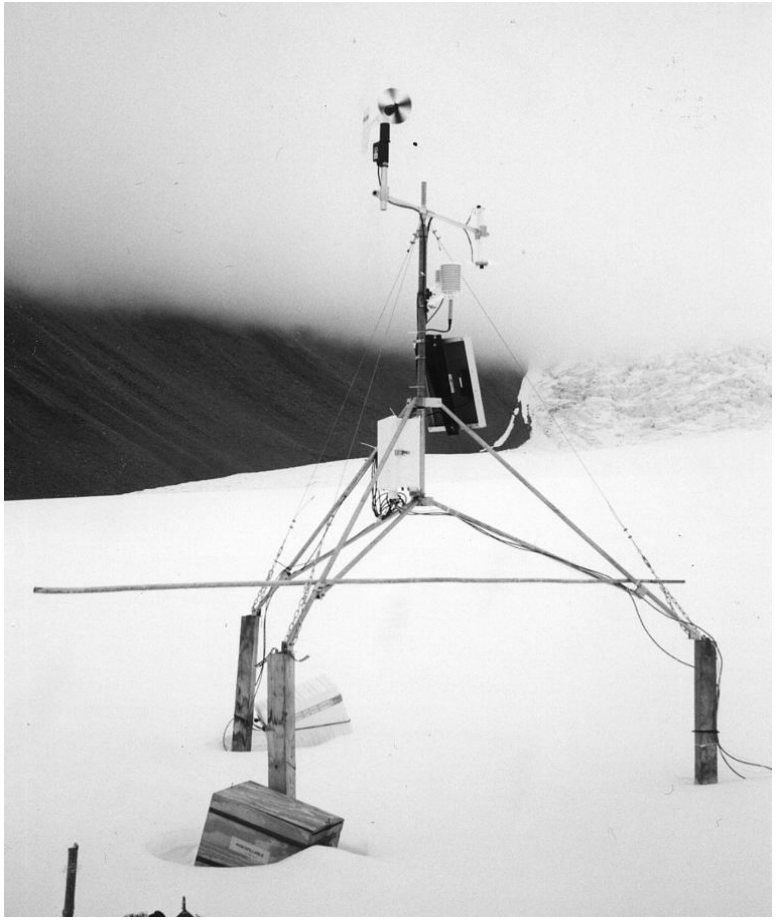

Figure 5: Canada Glacier meteorological station. Photo by Jonathan Ebnet, 2005.

Surface Mass Balance Data

Mass balance measurements are collected on Canada, Commonwealth, Howard (since 1993-1994), and Taylor glaciers (since 1994-1995). The height change of the snow or ice surface measured against stakes drilled vertically into the ice or snow is used to determine mass balance (Figure 6 and 7). The density of the surface material is measured if it is snow. The stakes are measured twice a year in early November and late January to determine the winter and summer mass balance (Fountain and others, 1994). The summer balance measurements in the ablation zone

were used to constrain the melt calculation, such that local estimated melt could not exceed measured ablation.

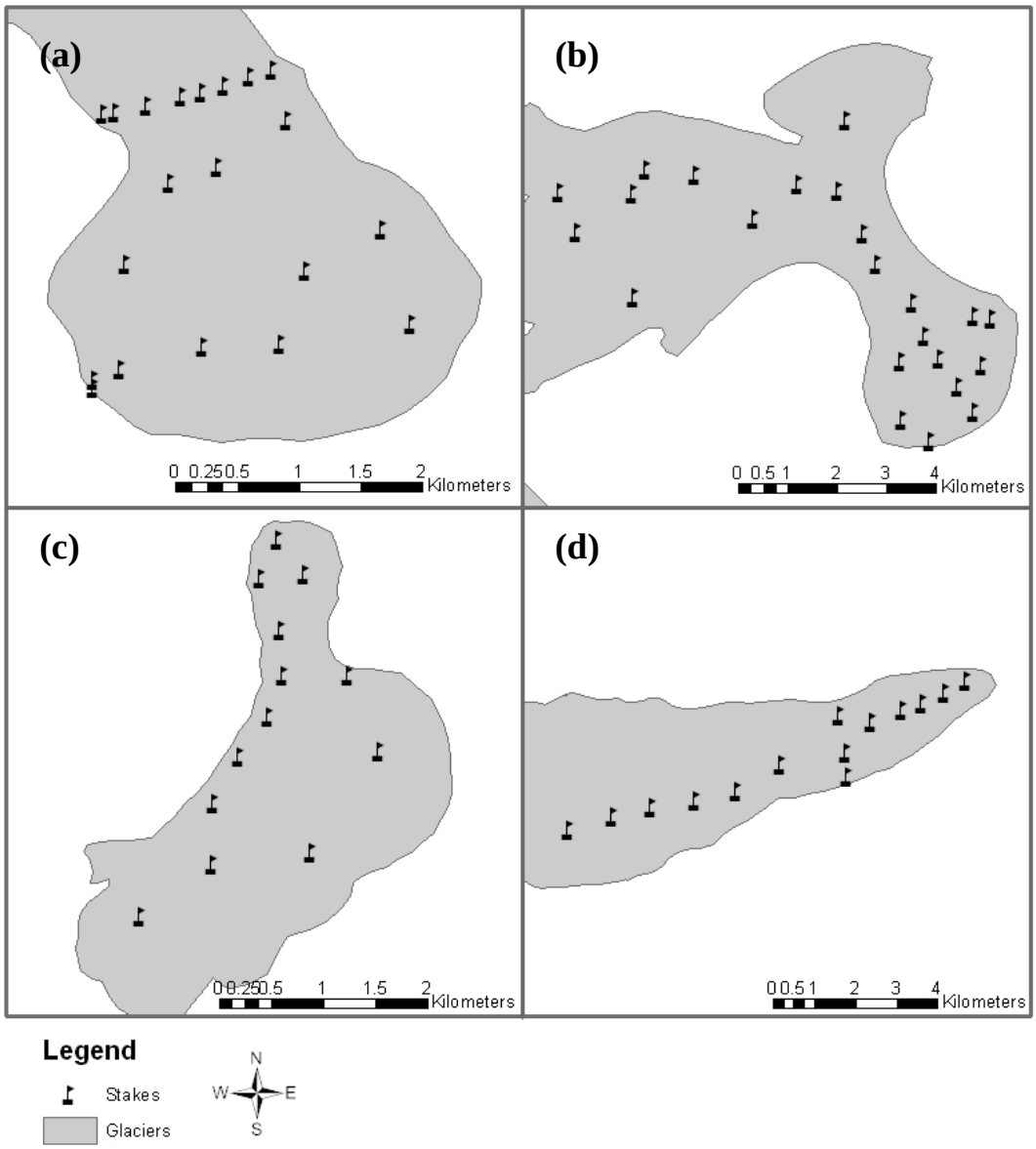

Figure 6: Mass balance stake locations for (a) Canada, (b) Commonwealth, (c) Howard and (d) Taylor glaciers (Fountain, accepted). Note the difference is scale. Only the ablation zone is measured on Canada and Taylor glaciers.

Figure 7: Ablation stake measurement on Canada Glacier. Photo by Thomas Nylen 2003-2004 season.

Correlations of Temperature with Stream Flow

To examine the relationship between stream flow and air temperature, monthly values of stream volume (November, December, January and February) from five glaciers in Taylor Valley (Canada, Commonwealth, Howard, Rhone and Taylor) were plotted against monthly air temperatures from the Lake Hoare meteorological station. For all cases except Taylor Glacier, the trend between temperature and stream flow shows a gradual increase in stream flow with increase in temperature at low temperatures. Once the average temperature reaches about -1.5 °C, the slope of the trend increases sharply. Polynomial and exponential equations were fit to the monthly total stream volume and air temperature data by least squares and Marquardt-

Levenberg methods to determine the best form of equation to use for the model. The Marquardt-Levenberg method is an iterative technique for finding the best-fit parameters for a nonlinear equation. The method works by making an initial guess of the parameter values and calculating the sum of squared differences between the observed and predicted data. The parameters are then adjusted in each iteration to decrease the sum of squared differences until they no longer decrease significantly (Bates and Watts, 1988). Good fits could not be found using first, second and third order polynomials (Figure 8).

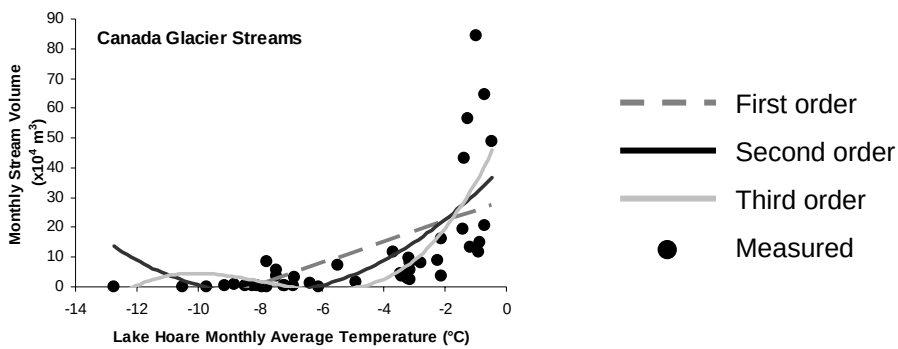

Figure 8 Polynomial regressions between monthly total stream volume from Canada Glacier and monthly average air temperature at Lake Hoare.

The quality of fit was assessed with the coefficient of determination and the p-value. The coefficient of determination,

$$r^2 = \frac{\sum(Q_m - \overline{Q}_m)^2 - \sum(Q_m - Q_c)^2}{\sum(Q_m - \overline{Q}_m)^2} \tag{5}$$

where, Q_m and Q_c are the measured and calculated stream flow volume respectively and $\overline{Q}_m$ is the mean measured stream flow volume (McClave and Sincich, 2000) increases while the p-value decreases with increase in order of the polynomial

equation (Table 2). The first order equation fails to depict the steep increase in stream volume at temperatures above -1.5°C. The second and third order polynomials perform better but still do not fit the highest three or four data points. The second and third order equations also causes the regressions to have a negative slope, which represents a decrease in stream flow volume with increase in temperature for a small range in temperatures, which is not representative of the trend in the data.

To capture the steep increase in stream volume at warmer temperatures an exponential equation of the form

$$Runoff = ae^{(bTemp)} + c \tag{6}$$

was tried (Figure 9). The coefficients *a* and *b* in (6) control the curvature of the function and *c* controls the horizontal asymptote. This allows the regression to fit the rapid rise in stream volume much better than the polynomials (Figure 9). The exponential equation yielded higher r^2 values and lower p-values than the polynomial equations (Table 2). The poor fit for Taylor Glacier may be due to poor stream data.

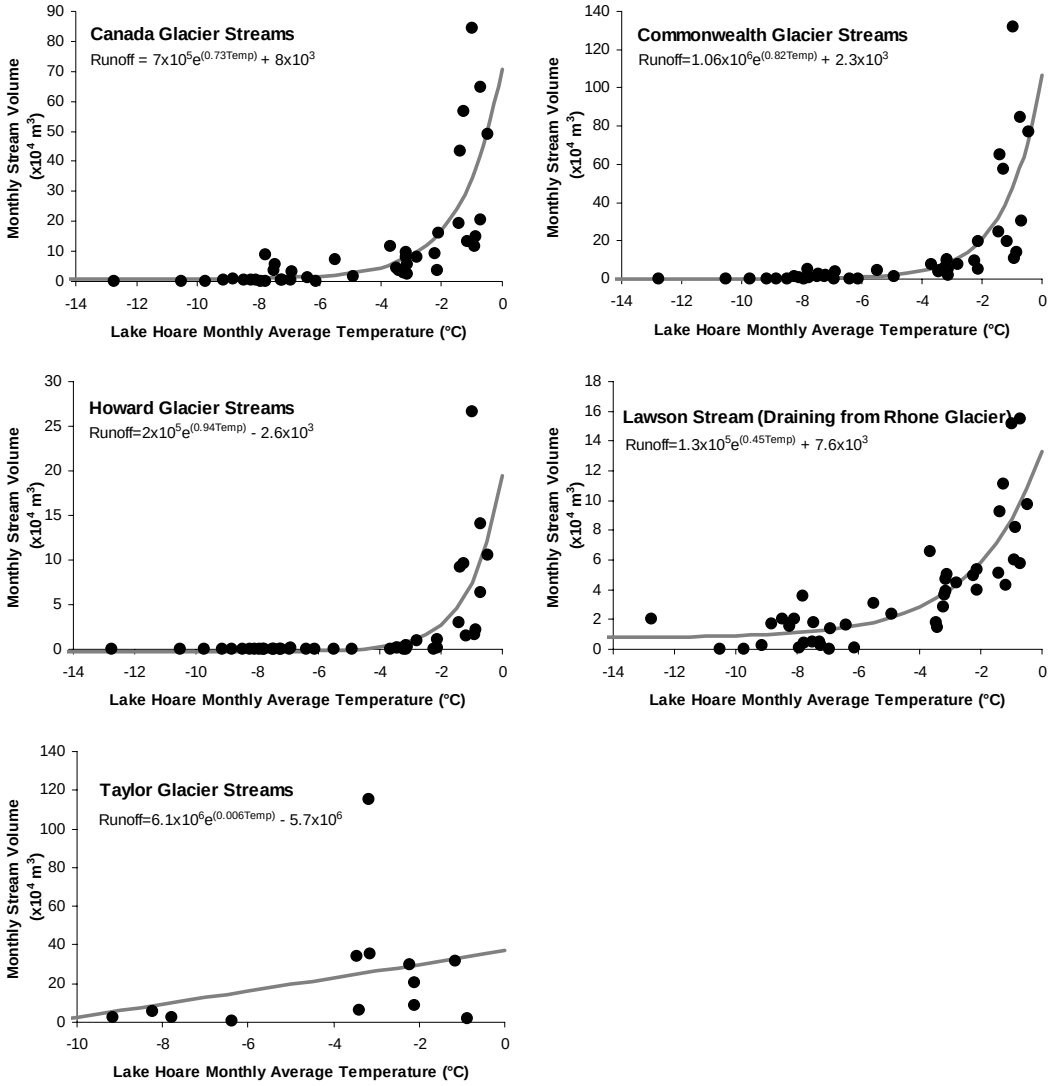

Figure 9: Exponential regressions between monthly total stream volume from the glaciers and monthly average air temperature at Lake Hoare. Note the difference in scale.

Table 2: Regression r^2 and p-values for monthly stream volume and air temperature.

Glacier	Regression	r^2	p-value
Canada	1st Order	0.37	1.7×10^{-05}
	2nd Order	0.50	1.0×10^{-06}
	3rd Order	0.57	2.2×10^{-07}
	Exponential	0.58	2.7×10^{-09}
Commonwealth	1st Order	0.33	5.2×10^{-05}
	2nd Order	0.47	3.1×10^{-06}
	3rd Order	0.55	5.6×10^{-07}
	Exponential	0.57	6.0×10^{-09}
Howard	1st Order	0.24	8.3×10^{-04}
	2nd Order	0.38	7.4×10^{-05}
	3rd Order	0.48	1.1×10^{-05}
	Exponential	0.48	2.2×10^{-07}
Rhone	1st Order	0.55	1.6×10^{-08}
	2nd Order	0.68	1.4×10^{-10}
	3rd Order	0.70	2.9×10^{-10}
	Exponential	0.70	2.3×10^{-12}
Taylor	1st Order	0.10	2.9×10^{-01}
	2nd Order	0.21	3.1×10^{-01}
	3rd Order	0.29	3.5×10^{-01}
	Exponential	0.10	3.0×10^{-01}

The seasonal stream volume is dominated (94%) by flow in December and January (Figure 10). Therefore, the months of November and February may be dropped from the model with little error (except for November 1997) in the estimate of total annual stream volume.

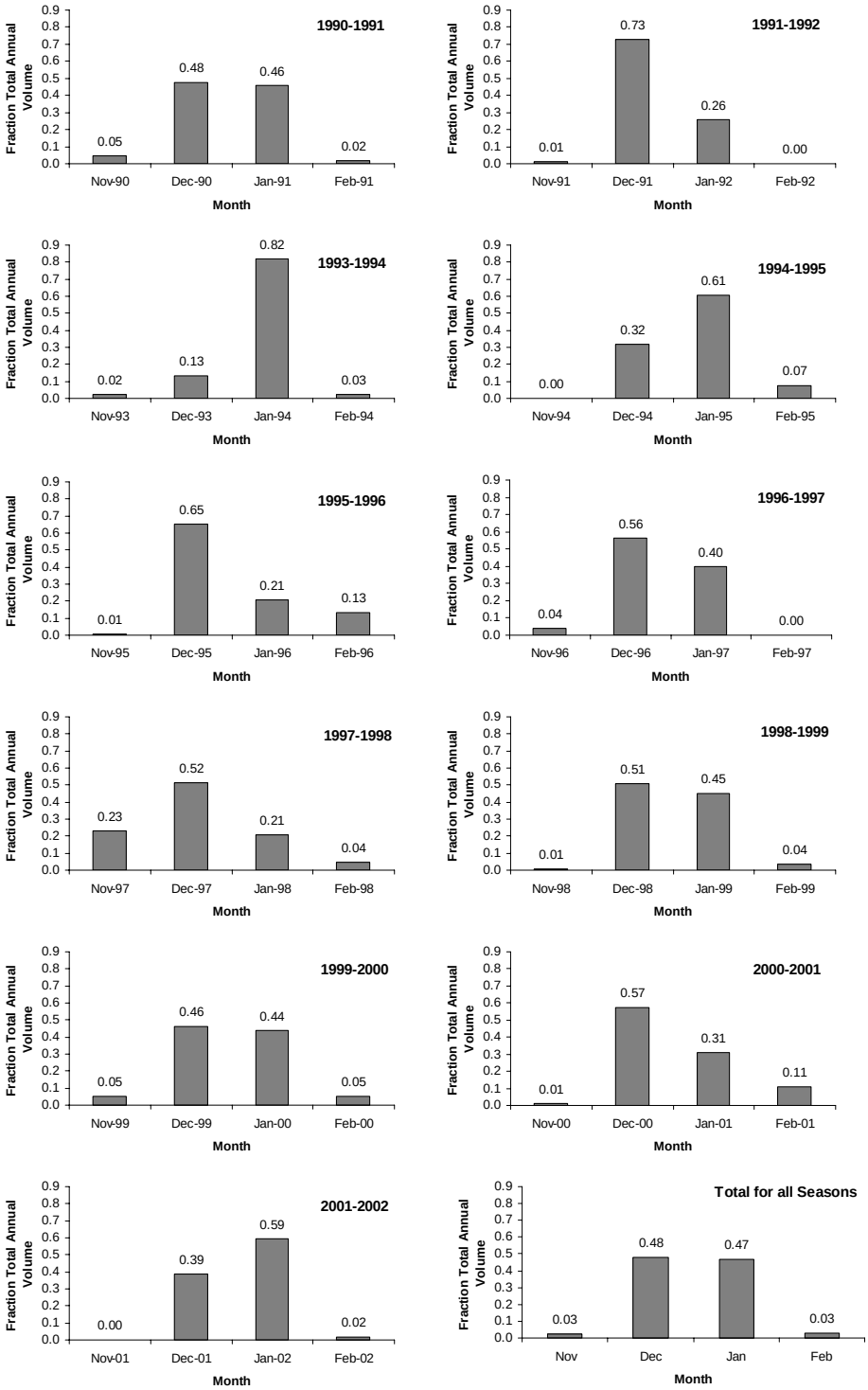

Figure 10: Stream hydrographs showing total stream volume from all thirteen streams.

The average air temperature at Lake Hoare for the months of November and February are -7.4°C and -8.2°C respectively, whereas the average temperature for the months of December and January are -2.0°C and -2.3°C respectively. Discarding the November and February values reduces the range of temperature over which stream flow is compared. An exponential function fit to the December and January data resulted in curve fits (Figure 11) that had lower r^2 values and higher p-values (Table 3) compared to the curve fit based on November through February values. The statistics for December and January data are worse than for November through February because the range of temperatures is smaller while the scatter at the warmer temperatures remains constant. The scatter in the December and January data is probably a result of non-temperature-related variations such as snowfall, cloud cover and wind. These influences will be discussed in Chapter 6.

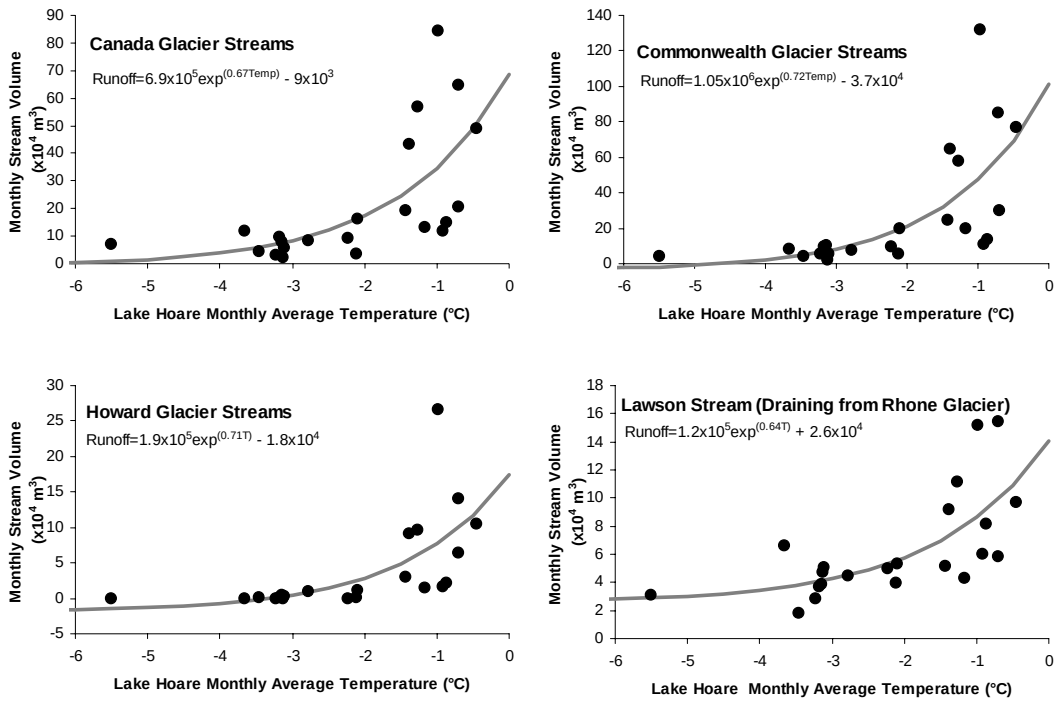

Figure 11: Exponential regressions through monthly stream volume and Lake Hoare air temperature for streams flowing from Canada, Commonwealth, Howard and Rhone glaciers excluding November and February. Note the changes in scale.

Table 3: Coefficients of determination and p-values for exponential regressions between monthly stream volume and Lake Hoare air temperature excluding November and February.

Glacier	r^2	p-value
Canada	0.43	9.3×10^{-4}
Commonwealth	0.43	8.6×10^{-4}
Howard	0.40	1.7×10^{-3}
Rhone	0.46	4.9×10^{-4}

To determine a seasonal trend between air temperature and stream volume, I totaled the stream volume over December and January and averaged the December and January air temperatures (Figure 12). The exponential regression through the seasonal data yielded much higher coefficients of determination and lower p-values (Table 4). Because my goal is to estimate total seasonal stream flow and because

summer values correlate better than monthly values, I use the summer values in the model. From this point on, summer refers to December through January.

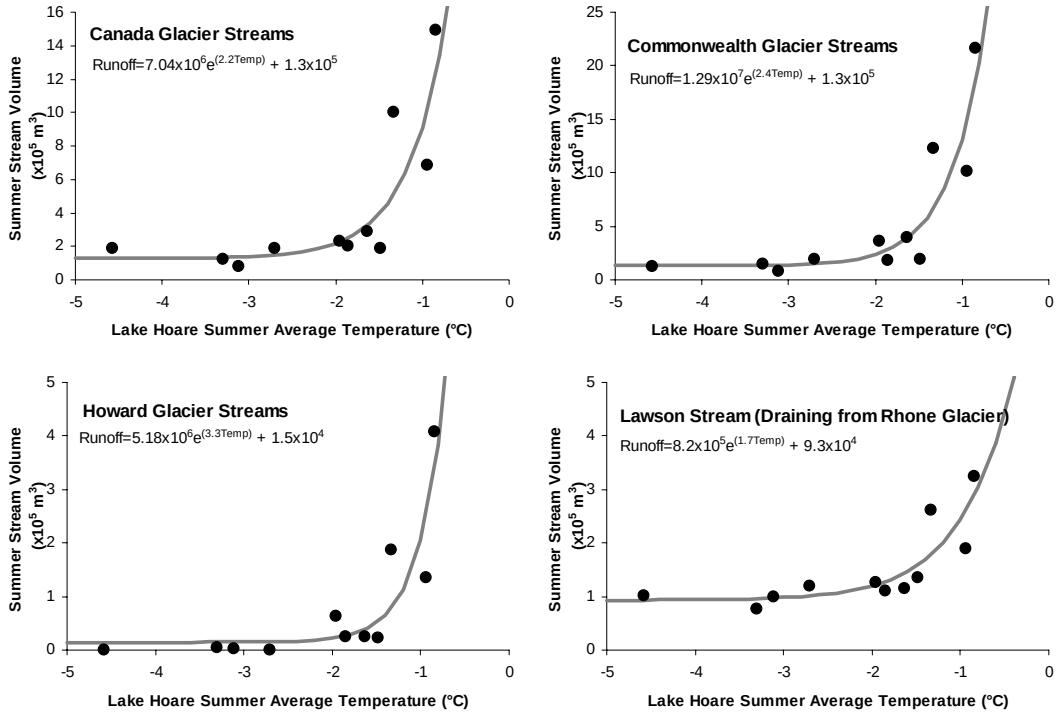

Figure 12: Exponential regressions through summer stream volume (totaled for the months of December and January) and Lake Hoare air temperature (averaged over the months of December and January) for streams flowing from Canada, Commonwealth, Howard and Rhone glaciers. Note differences in scale.

Table 4: Coefficients of determination and p-values for exponential regressions between seasonal stream volume and Lake Hoare air temperature.

Glacier	r^2	p-value
Canada	0.77	5.4×10^{-4}
Commonwealth	0.82	1.2×10^{-4}
Howard	0.79	2.5×10^{-4}
Rhone	0.74	6.6×10^{-4}

To estimate the total melt-water flux into the lakes I need to estimate stream flow in ungauged streams and, where glaciers contact the lakes, flux directly from the

glaciers to the lakes. Therefore, I need to estimate ice melt rather than stream flow directly. This approach is useful for estimating stream flow in past glacial conditions, where the distribution of glacier area may be different from today. This is also useful for estimating stream flow for glaciers with different area – elevation distributions (Figure 13). The results from this chapter provided important information on the temperature-melt (expressed as stream flow) relation for the stream flow model.

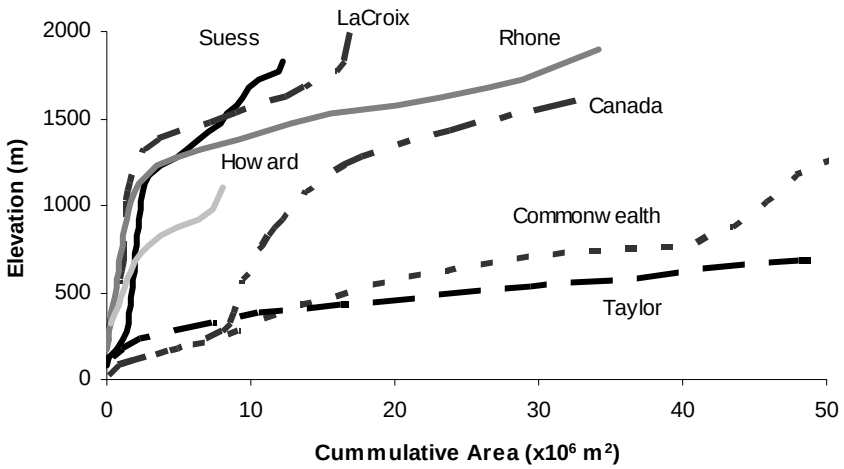

Figure 13: Area-elevation distribution of selected glaciers in Taylor Valley.

III STREAM FLOW VOLUME MODEL

Stream flow volume from each glacier is based on the total melt and contributing area by,

$$Q = \int_A M dA \tag{7}$$

where Q is the total seasonal stream flow volume and M is the total seasonal specific melt for each stream ($m^3 m^{-2}$) over the glacier area A. The integral over A may be approximated by,

$$Q = \sum M(T_{x,y,z}, I, U) A(z) \tag{8}$$

I choose M to be a function of three variables, temperature (T), which varies from summer to summer and is itself a function of location (x, y, z), solar radiation (I), which is constant in time but varies spatially, and wind speed (U), which also only varies spatially. As discussed earlier, M is most accurately calculated using a complete energy balance at the ice surface, but my intent is to predict melt, using as few variables as possible, during times prior to meteorological measurements in Taylor Valley. Temperature was chosen because it is a key variable in the energy balance and is highly correlated with melt. Solar radiation was chosen because of the large spatial differences in solar radiation received by the glaciers in the valley (Dana and others, 2002; Fountain and others, 1999). Wind is included because of its fundamental importance in the turbulent terms of the energy balance equation and its demonstrated influence on partitioning ice ablation between melt and sublimation (Johnston, 2004; Fountain and others 1999b; Lewis and others, 1998).

To account for temperature control on melting, the differences in temperature across the valley are first defined. The seasonal air temperature within Taylor Valley increases with distance from the coast (Doran and others, 2002) and from the center of the valley bottom toward the side (Delaney, Chad, written communication, 2003) as a result of warming over the exposed soil. Air temperature also decreases with elevation according to the adiabatic lapse rate (Doran and others, 2002). The spatial variation in summer average temperature is approximated by

$$T_{x,y,z} = 0.09x + 0.24y - 9.8z - T_0 \tag{9}$$

(Delany, Chad, written communication, 2003) where x is the distance from the coast, y is the distance from the valley bottom and z is the elevation (all in km) and T_o is the summer average temperature at the coast. The vertical gradient, -9.8 °C km^{-1}, is the dry adiabatic lapse rate, which is typical for Taylor Valley (Lewis and others 1998). The other gradients were determined by a least squares polynomial fit to the average summer air temperature measurements across the valleys from the 1997-1998 season. Equation (8) was modified to predict valley temperatures from the meteorological station at Lake Hoare, which has the longest running record,

$$T_{x,y,z} = 0.09(x - x_H) + 0.24(y - y_H) - 9.8(z - z_H) + T_H \tag{10}$$

where the subscript H indicates the value at Lake Hoare. Summer average air temperatures were calculated for seven other meteorological stations in the valley and compared to the measured summer average temperatures (Figure 14). All deviations

are less than 1°C, and many are less than 0.5°C. The coefficient of determination between measured and calculated air temperature is $r^2 = 0.95$.

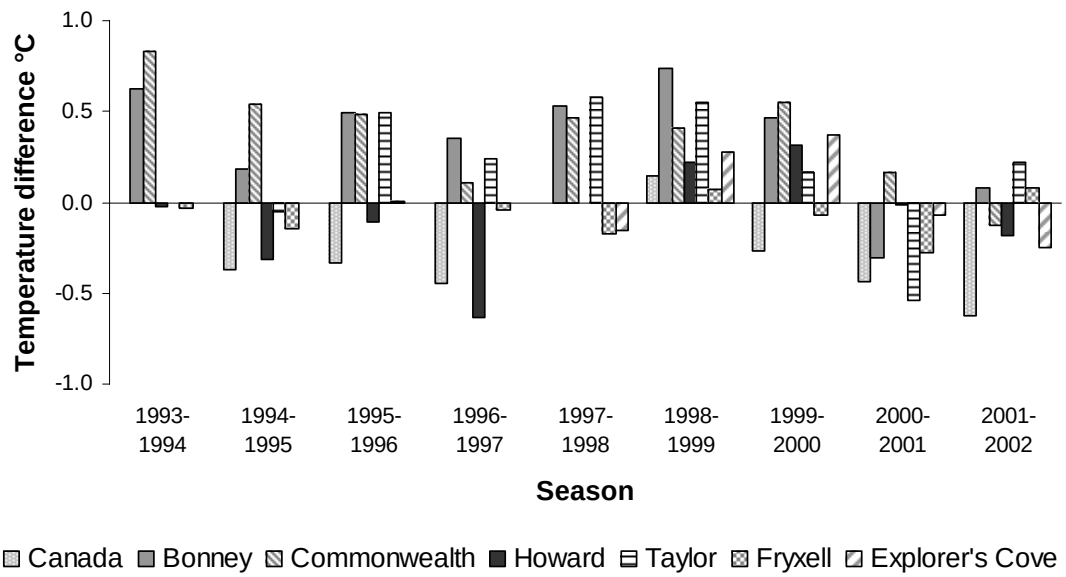

Figure 14: Residuals between modeled temperature and measured summer (December – January) temperature at the Taylor Valley meteorological stations. A positive difference indicates that the modeled temperature is greater than the measured.

Potential direct solar radiation, *I,* is calculated

$$I = I_0 \left(\frac{R_m}{R} \right)^2 \psi_a^{\left(\frac{P}{P_0 \cos \theta_Z} \right)} \cos \theta_I \tag{11}$$

(Hock, 1999) where I_0 is the solar constant (1368 W m^{-2}, Fröhlich (1993)), $\left(\frac{R_m}{R} \right)^2$ is the eccentricity correction factor where R is the instantaneous sun-Earth distance, and R_m is the mean sun-Earth distance, ψ_a is the mean atmospheric clear-sky transmissivity, P is the atmospheric pressure, P_0 is the mean atmospheric pressure at

sea level, θ_Z is the zenith angle (angle between vertical and the solar ray) and θ_I is the incident angle between the solar ray and the normal to the surface. Following Iqbal (1983), the eccentricity correction factor is

$$\left(\frac{R_m}{R}\right)^2 = 1.000110 + 0.034221\cos\Gamma + 0.001280\sin\Gamma + 0.000719\cos 2\Gamma + 0.000077\sin 2\Gamma \tag{12}$$

$$\Gamma = \frac{2\pi(J-1)}{365} \tag{13}$$

where Γ is the day angle (in radians) and J is the Julian Day. The incident angle of the solar ray and earth surface is calculated

$$\cos\theta_I = \cos\beta\cos\theta_Z + \sin\beta\sin\theta_Z\cos(\varphi_{sun} - \varphi_{slope}) \tag{14}$$

where β is the angle of the surface slope from horizontal, θ_Z is the zenith angle, φ_{sun} is the solar azimuth (the angle at local zenith between the plane of the observer's meridian and the plane of a great circle passing through the zenith and the sun), and φ_{slope} is the aspect of the surface (Figure 15).

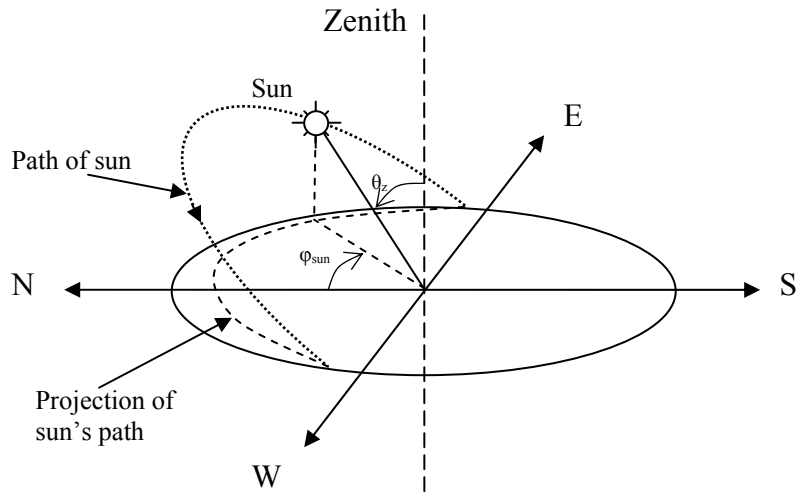

Figure 15: The sun's zenith and azimuth angles. Adapted from Iqbal, (1983).

The zenith angle is a function of latitude, solar declination and hour angle. The hour angle is the angle measured at the celestial pole between the observer's meridian and the solar meridian. The solar declination (δ) is the angle between a line joining the centers of the sun and earth at solar noon and the equatorial plane. The solar declination for a given day is

$$\begin{aligned}\delta = {} & 0.006918 - 0.399912\cos\Gamma + 0.070257\sin\Gamma \\ & - 0.006758\cos 2\Gamma + 0.000907\sin 2\Gamma \\ & - 0.002697\cos 3\Gamma + 0.00148\sin 3\Gamma\end{aligned} \tag{15}$$

with a maximum error of 0.0006 radians. The zenith angle can be calculated

$$\cos\theta_Z = \sin\delta\sin\phi + \cos\delta\cos\phi\cos\omega \tag{16}$$

where ϕ is the geographic latitude (-77°40′) and ω is the hour angle where noon is 0°, morning is positive and a one hour increment is 15° (Figure 16). Finally the solar azimuth is calculated

$$\cos\varphi_{sun} = \frac{(\sin(90-\theta_z)\sin\phi)-\sin\delta}{\cos(90-\theta_z)\cos\phi} \tag{17}$$

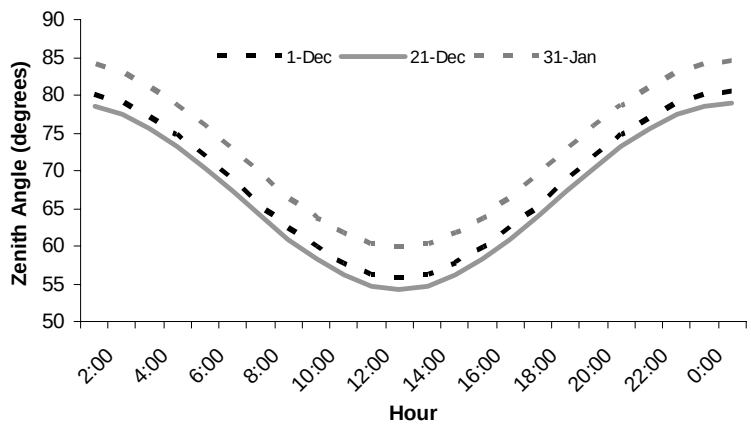

Figure 16: Zenith angle as a function of hour for December 1, December 21 and January 31.

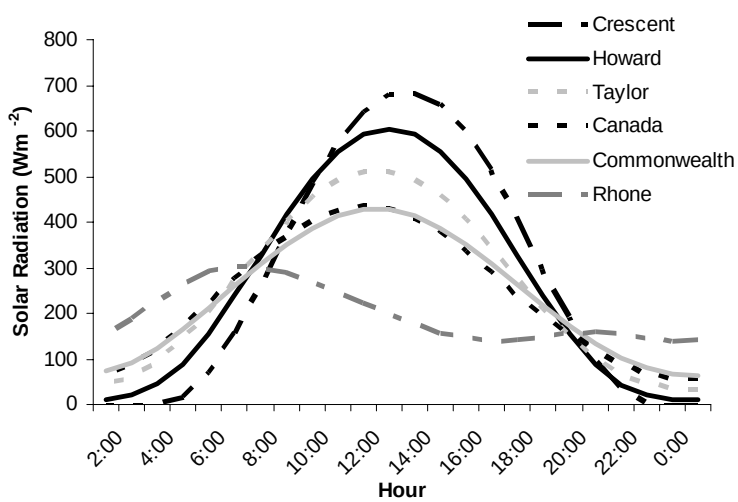

Figure 17: Hourly solar radiation calculated on the summer solstice (December 21) and averaged over the ablation area of selected glacier.

Slope and aspect were measured at points 50 m in elevation apart along the center of the ablation zone of each glacier. The potential solar radiation was calculated at each point at hourly intervals from December 1 to January 31. For the hours when the sun drops below the plane of the glacier surface, potential solar radiation was set to zero. No effect of shadowing by surrounding terrain was included. The results were averaged over time then over the surface of the glacier, yielding a single solar radiation value for each glacier (Table 5).

The summer average wind speed (U) was calculated by averaging the summer wind speed over all years of record for each meteorological station in the valley (Table 5). The wind regime was estimated by means of an ordinary kriging method in which an ellipse defined the kriging domain for Taylor Valley, and wind speeds were estimated using the nearest two to four meteorological stations (Delany, Chad, personal communication, 2004).

Table 5: Solar radiation and wind speed for glaciers.

Glacier	**Solar Radiation ($W\ m^{-2}$)**	**Average Wind Speed ($m\ s^{-1}$)**
Canada	242	3.2
Commonwealth	243	3.5
Howard	266	2.7
Crescent	275	3.0
VonGuerard	279	3.2
Taylor	257	4.5
Rhone	210	4.3
LaCroix	221	3.8
Suess	214	2.7

IV MODEL APPLICATION

Temperature-Index Model

To estimate total melt-water contribution to the lakes, I start with the temperature-index model then examine the temperature-solar radiation model and finally the temperature-solar radiation-wind model. Many temperature-index models (hereafter, T-model) are based on a linear relationship between air temperature and melt $M = f(T_{x,y,z})$ (Hock, 1999; Kane and Greck, 1997; Braithwaite, 1995; Kustas and Rango, 1994). As discussed previously, plots of summer stream flow volume and summer average temperature in Taylor Valley clearly show a non-linear relationship that is well approximated by an exponential function.

$$M = Ae^{(BT^*)} + E \tag{18}$$

where A, B and E are empirically-determined parameters. The constant E effectively prevents the calculation of melt below a threshold temperature (the lowest temperature at which melt occurs). T^* is the normalized air temperature (discussed below). Solar radiation is added to the temperature-index model to improve the melt prediction spatially. The temperature-solar radiation (TI) model is of the form

$$M = Ae^{B\left(T^* + CI^*\right)} + E \tag{19}$$

where I^* is normalized potential direct solar radiation on a glacier (discussed below) and C is an empirically-determined parameter. Finally a temperature-solar radiation-wind (TIU) model is given by the relation

$$M = Ae^{B\left(T^* + CI^* + DU^*\right)} + E \tag{20}$$

where U^* is normalized average wind speed for each glacier in Taylor Valley (discussed below) and D is an empirically-determined parameter.

Each glacier was divided into drainages bounded by the water flow divides to different valley streams, as defined by surface topography and expressed by elevation contours on topographic maps. The drainages were further subdivided by the 50 m elevation contours to account for the elevation change on the glacier in the calculation of air temperature (Figure 18, 19, 20, and 21). Summer average temperature was calculated at the midpoint of each section for the 11 seasons using equation (9). Melt was then calculated at the midpoints (equations 18 – 20) and multiplied by the surface area of the corresponding section yielding a melt volume. Stream volume for each drainage is the sum of the melt volumes over the surface of the drainage.

Normalized values of the independent variable were used in the TI and TIU models, (equations 19 and 20) to assess the relative importance of each variable and in the T-model for consistency with the other two models. The temperatures were normalized

$$T^* = \frac{T_{x,y,z} - \overline{T}_{x,y,z}}{S_T} \tag{21}$$

where $\overline{T}_{x,y,z}$ is a mean and S_T is a standard deviation of temperatures in the ablation zones of the glaciers in Taylor Valley. To calculate the mean and standard deviation of air temperature, air temperatures were calculated at the midpoint of the 50 m elevation intervals in the ablation zones from equation (9) of every glacier contributing melt to the three lakes in the valley for each of the eleven seasons of the model. The mean and standard deviation is calculated from all midpoints over the eleven seasons.

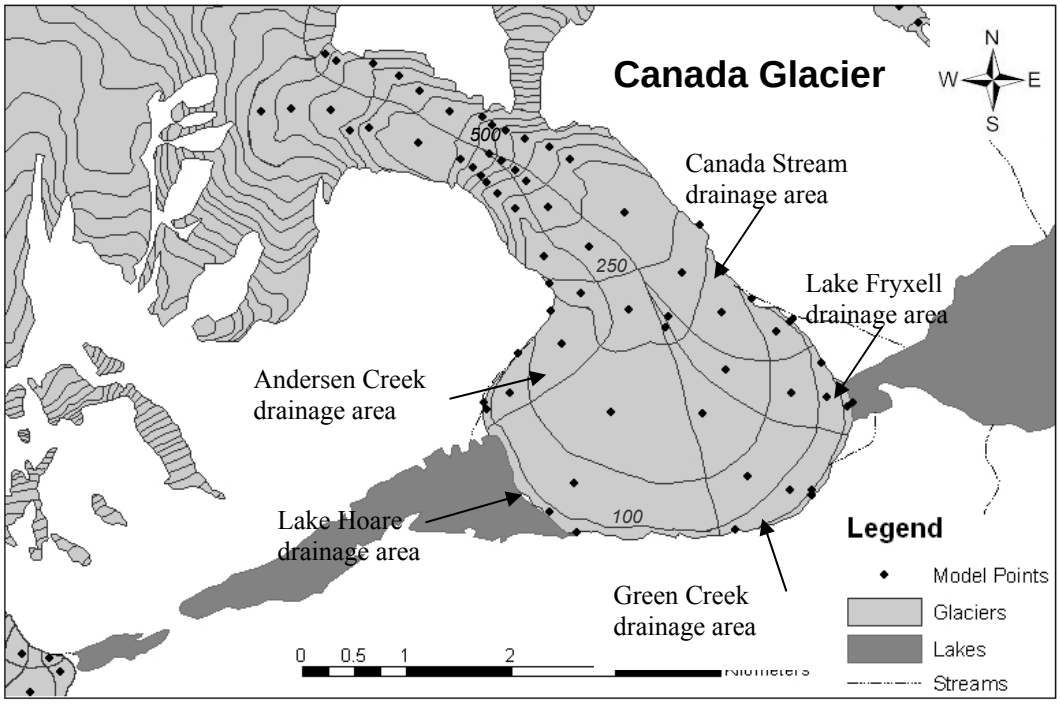

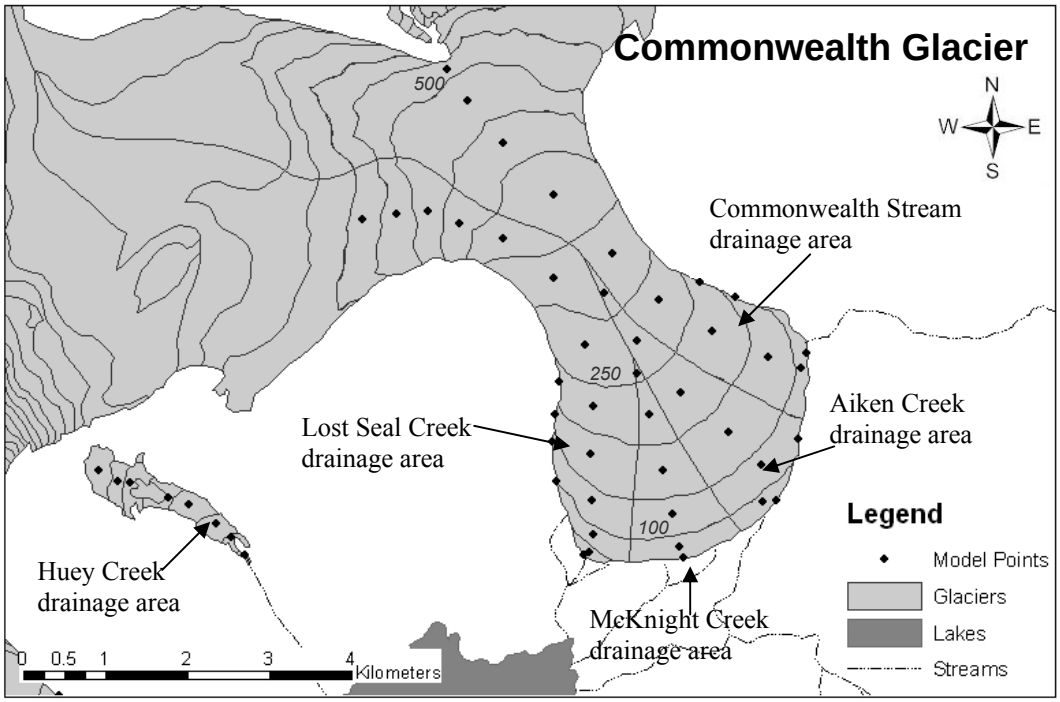

Figure 18: Glacier contributing areas and model calculation points for Canada and Commonwealth glaciers.

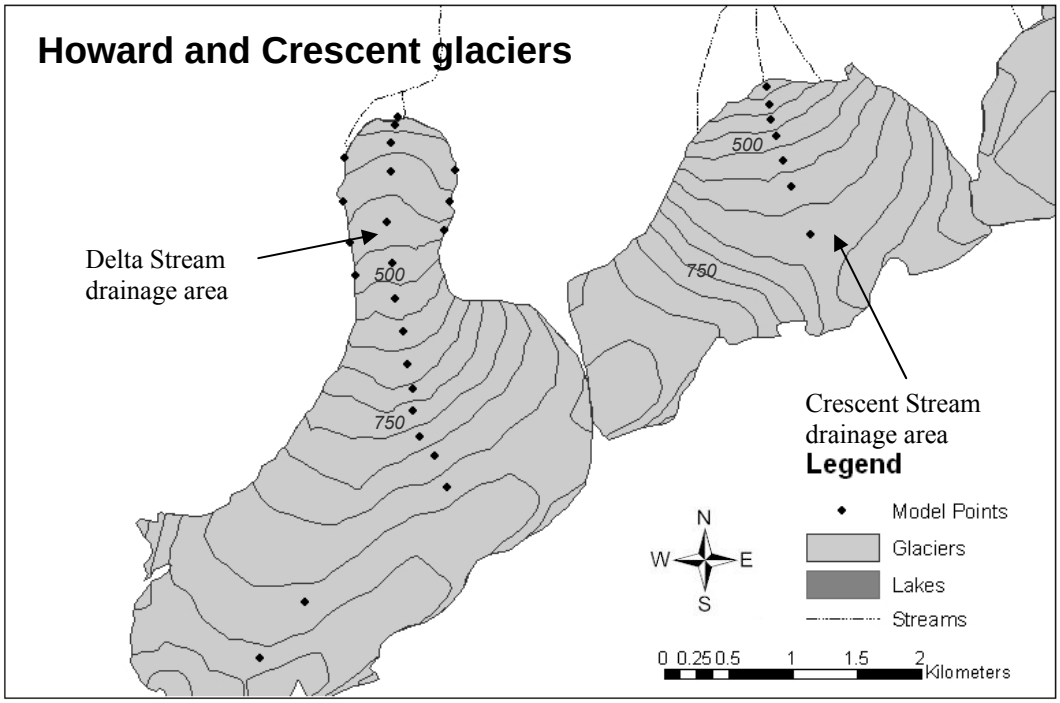

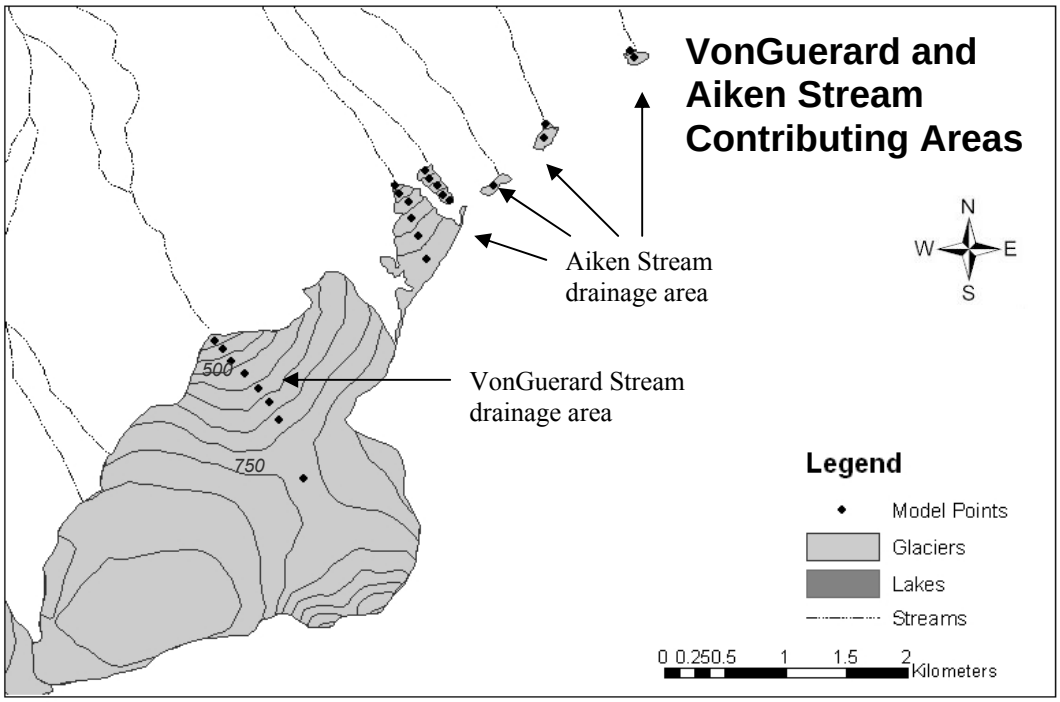

Figure 19: Glacier contributing areas and model calculation points for Howard and Crescent glaciers and VonGuerard and Aiken streams.

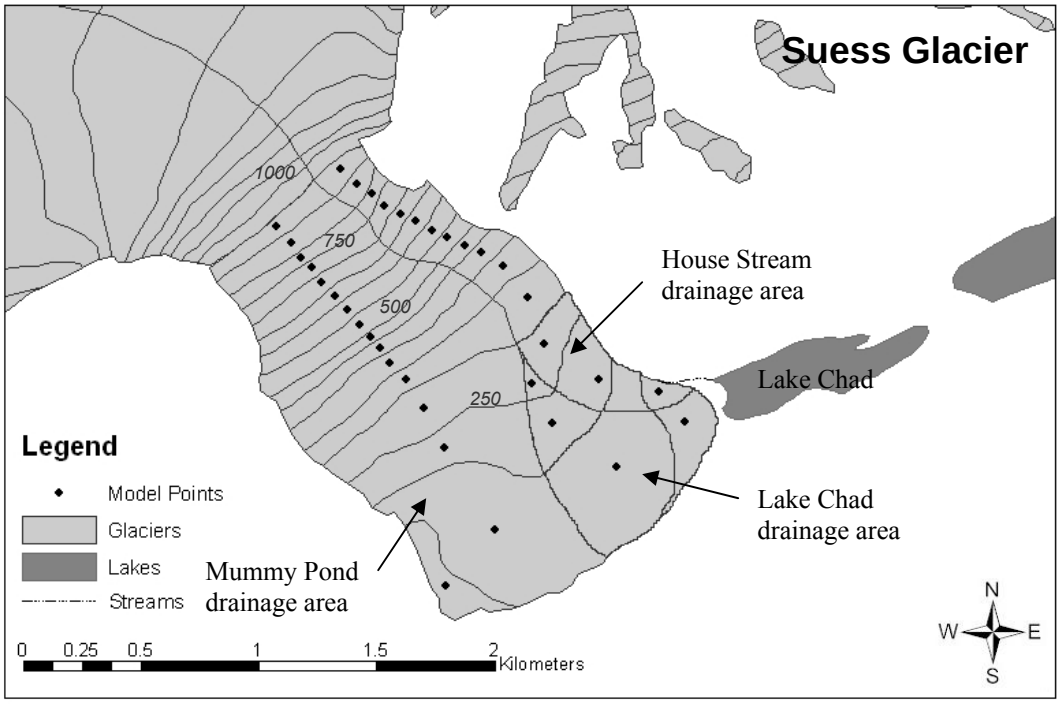

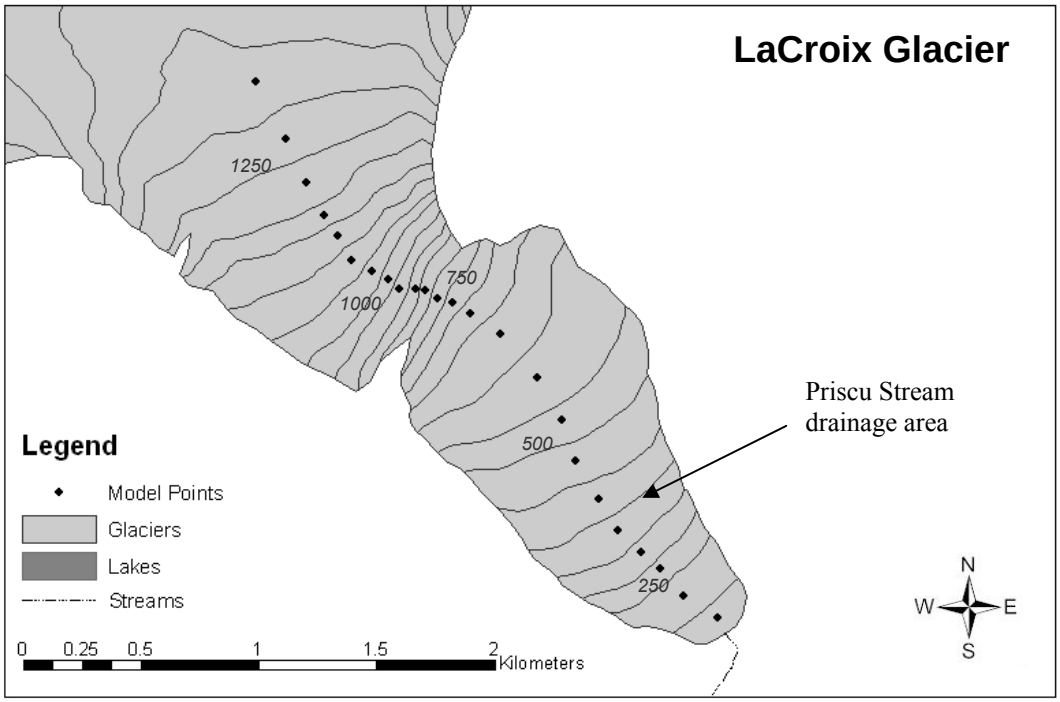

Figure 20: Glacier contributing areas and model calculation points for Suess and LaCroix glaciers.

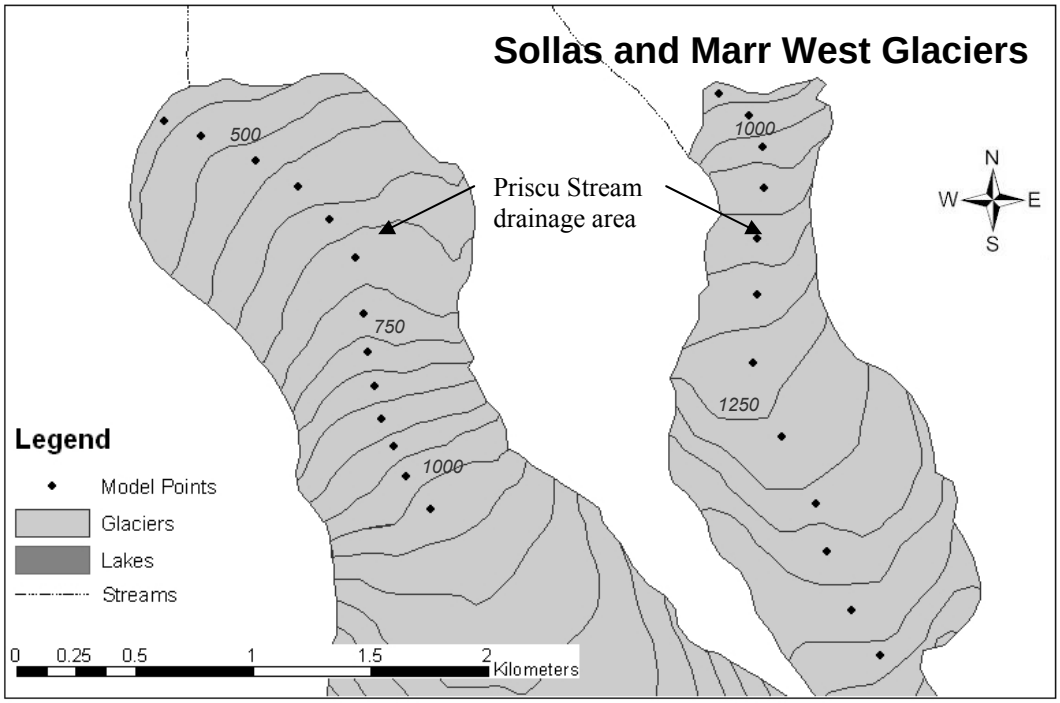

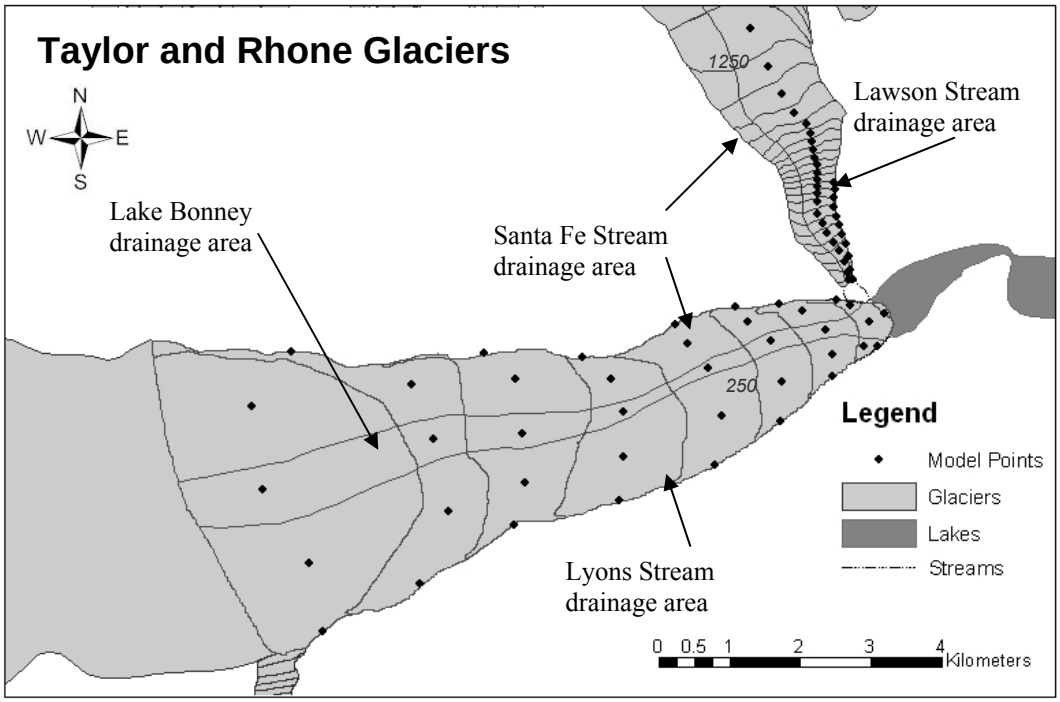

Figure 21: Glacier contributing areas and model calculation points for Sollas, Marr West, Taylor and Rhone glaciers.

For the TI model, the potential direct solar radiation was calculated at the midpoint of each elevation interval on the glacier and averaged over the ablation zone of each glacier. The average solar radiation value for each glacier ablation zone was normalized using the average and standard deviation of all glaciers in the valley

$$I^* = \frac{I - \bar{I}}{S_I} \tag{22}$$

where $\bar{I}$ and S_I are the mean and standard deviation of the solar radiation values of all the glaciers, respectively.

For the TIU model, the summer average wind speed over all seasons and over each glacier is normalized over all glaciers in the valley

$$U^* = \frac{U - \overline{U}}{S_U}. \tag{23}$$

The mean ($\overline{U}$) and standard deviation (S_U) of the wind speed for all glaciers was calculated from summer average wind speed over all glaciers in the model.

Threshold Temperature and Melt Limit

As temperature decreases with increasing elevation, calculated melt decreases to zero when the temperature drops below a threshold value. The threshold temperature for melt (T_m) is the summer average temperature below which no melt occurs. This temperature is derived from the models by setting M in equation (19) to zero and solving for T,

$$T_m = \frac{\ln(E/A)}{B} - CI - DU \tag{24}.$$

The coefficients D and C are set to zero for the T-model and D is set to zero for the TI-model. The melt limit is the elevation at which the threshold temperature occurs according to the lapse rate. T_m is constant and is the same for every glacier in the T-model. The melt limit, however, varies from glacier to glacier because temperatures increase with distance from the coast and the valley bottom. For the TI and TIU-models, T_m remains constant seasonally but varies spatially among glaciers due to the local effects of solar radiation and wind-speed. This also increases the variability in melt limit among glaciers.

Cliff Melt

Vertical cliffs commonly form the lower margin of the glaciers in Taylor Valley. Attempts were made to incorporate cliff aspect and shading into the models with little success because of the complexities of the enhanced melt on the cliffs. Instead, cliff melt (M_c) was calculated separately from surface melt using a separate temperature-index model,

$$M_c = ae^{\left(bT_{x,y,z}\right)} + c \tag{25}$$

where a = 0.48 m, b = 0.3 °C^{-1}, and c = -0.026 m, as I determined from the regression fit to measured ablation on the cliffs of Canada Glacier (data obtained from http://huey.colorado.edu). I applied equation (25) to all glacier cliffs in the valley. The total volume of cliff melt was then calculated as the product of cliff melt and cliff area. The area was determined by measuring the cliff length between the 50 m contours in ArcMap and multiplying it by the cliff height measured on a LIDAR high-

resolution digital elevation model. Where measurements were not available, cliff height was assumed to be 20 m. The total melt from the cliffs was then added to the total runoff over the glacier surface (equation 8).

Stream Evaporation

Few of the stream gauges are located near the point where water runs off the glacier. The gauges on some streams (e.g. Delta) may be several kilometers from the source. In these conditions evaporative stream losses can be important. Because our goal is to predict water flow to the lakes, it is important to define evaporative stream losses. Evaporation loss is estimated as a function of stream length and width. That is, a relatively longer and wider stream suffers relatively larger losses than narrower shorter streams. Evaporation pan experiments yield summer evaporative rate of 7.14×10^{-8} $m^3 m^{-2} s^{-1}$ of water (Gooseff and others, 2003). To obtain volume loss, the specific loss rate is multiplied by the stream length and width and the length of the melt season (two months).

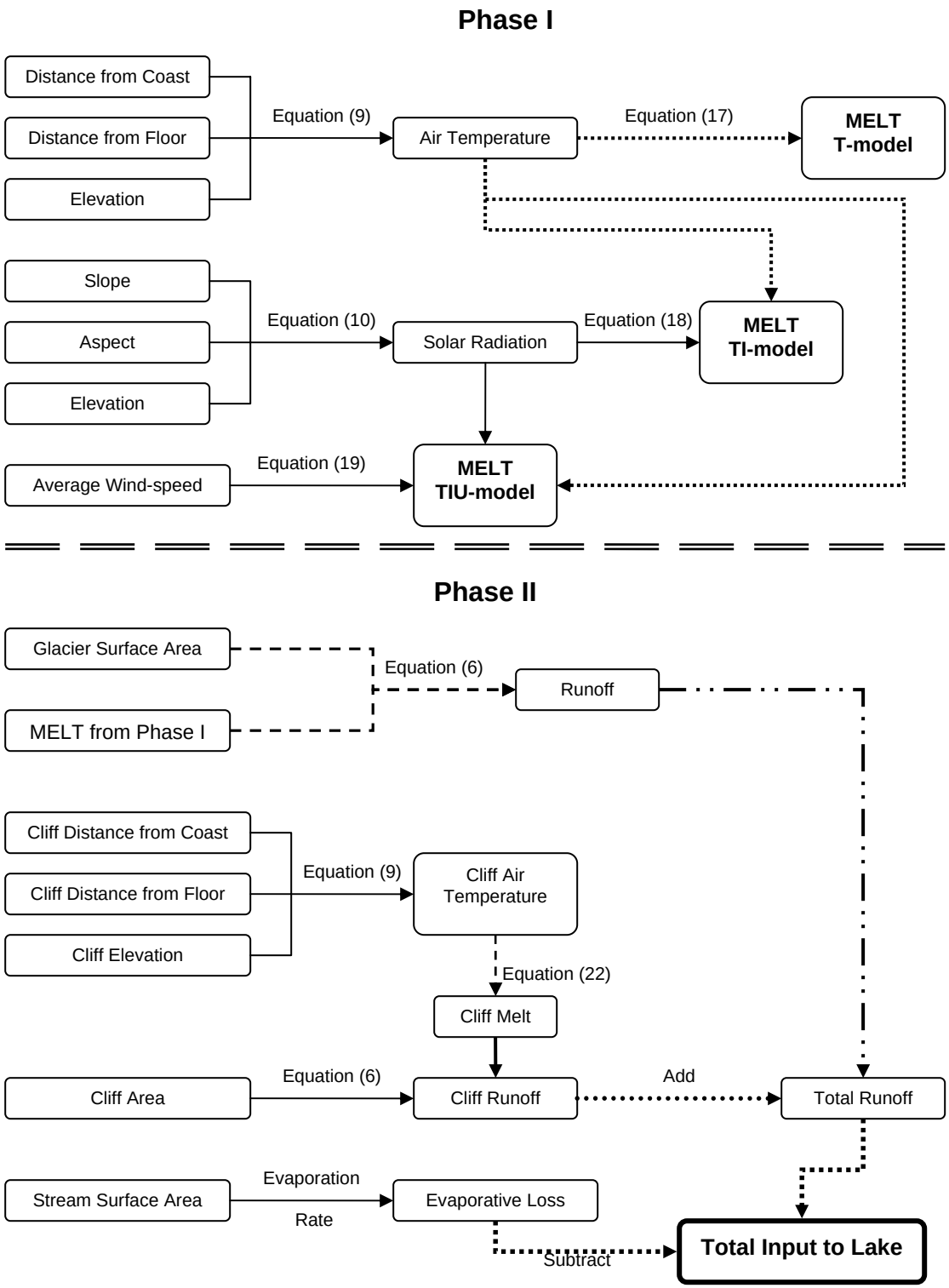

Figure 22: Model flow chart.

Model Calibration

The models cannot be fit directly to observed stream flow volume because of the summation in equation (8). Melt limits and thus the contributing areas of the glaciers depend on the empirically-derived coefficients in the melt equations. So the models are fit to measured ablation and then compared to measured stream flow volume. The coefficients for each melt model were determined by fitting equations (17-19) to the measured ablation from Canada, Commonwealth, Howard, and Taylor glaciers using the Marquardt-Levenberg method in PSI-PLOT software. Sublimation makes up a significant proportion of ablation (40-80%) from the glaciers (Lewis and others 1998). To account for the fraction of ablation attributed to sublimation, the ablation data were divided in half before fitting. There is much uncertainty in the magnitude of sublimation and attributing half of the ablation to sublimation is only a rough value.

The parameter values which provide a best fit for the melt data might not produce the best fit for the stream volume. For instance, stream volume was calculated by equation (6) using the melt calculated from the T-model, equation (18), with the best fit parameter values for Canada Glacier and compared to the measured stream volume from Canada Glacier. While the results of the curve fit worked well for the melt calculation, stream volume was significantly underestimated for the warm years (Figure 23).

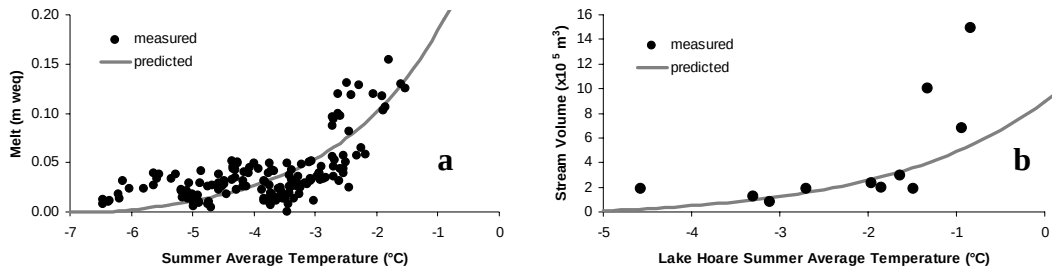

Figure 23: Curve fit to the measured melt (ablation reduced by half) on Canada Glacier (a) and the resulting curve for stream flow volume from Canada Glacier compared to the total measured stream flow volume from Andersen, Green and Canada streams (b).

The coefficients *A* and *B* were adjusted to improve the calculated stream volume curve. The solar and wind terms represent the spatial and not temporal variations in melt and stream flow so changing C and D will not improve the stream flow results for the warm years. The estimated melt with the new coefficients are compared to the measured ablation to ensure that modeled melt does not exceed measured ablation.

The coefficients for the models were adjusted to best fit the stream flow volume data from as many streams as possible. Small changes in the coefficients can produce drastically different results. Changes in *A* and *B*, in the T-model have the largest effect at warmer temperatures (Figure 24).

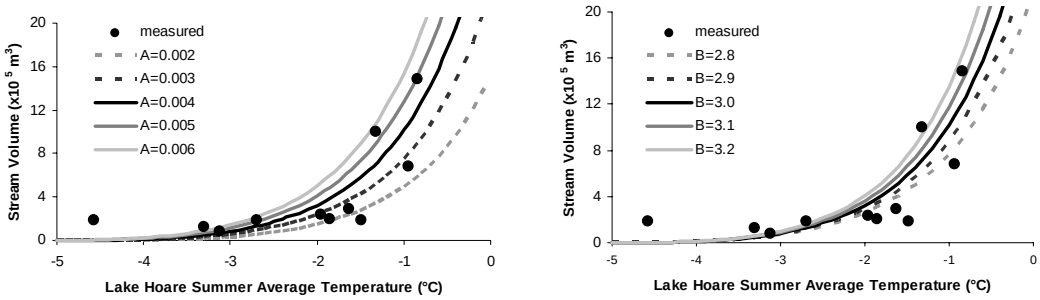

Figure 24: Sensitivity of T-model to (a) variations in the *A* coefficient compared to measured stream flow volume from Canada Glacier. The coefficient *B*=3.0. And sensitivity to (b) variation in the *B* coefficient compared to measured stream flow volume from Canada Glacier. The coefficient *A*=0.004.

Model accuracy is evaluated using the coefficient of determination (r^2 value) (McClave and Sincich, 2000), which indicates what fraction of the variability in stream flow volume is accounted for by the model. Negative r^2 values indicate the variability in the difference between measured and calculated stream flow volume is larger than the variability in the measured stream flow volume. The total error in volume summed over the eleven summer seasons was calculated by dividing the difference between total calculated and measured stream volume by the total measured stream volume.

The parameter values which provide a best fit for stream volume from Canada Glacier may not produce a good fit for other glaciers. The best fit T-model for Canada Glacier (*A*=0.004, *B*=3.0) results in a poor fit for Howard Glacier (Figure 25A). Howard Glacier is a north-facing glacier and receives more solar radiation than the south facing Canada Glacier. Applying the TI model, using the same *A* and *B* values and including a non-zero value for *C* in equation (19) shifts the stream flow volume (and melt) curves along the temperature axis. The normalized solar radiation index

term is 0.49 for Howard Glacier and -0.40 for Canada Glacier. With a positive coefficient *C* the stream flow volume curve shifts towards colder air temperature for Howard Glacier resulting in an increase in the melt at colder air temperatures relative to Canada Glacier. As shown in Figure 25, increasing *C* from 0 to 0.5 shifts the curve from a to b. Increasing *C* even further to *C*=1 shifts the results to curve c making a close fit to the measured data for Howard Glacier, but increases the error for Canada Glacier. By adjusting both A and B, a reasonable fit to the stream flow volumes of both glaciers is possible (d).

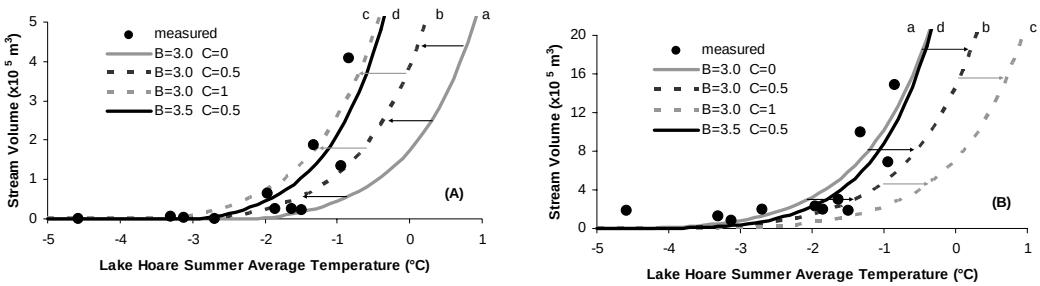

Figure 25: Sensitivity of incorporating the solar radiation index in the TI-model and of changes in the *C* coefficient for (A) Howard Glacier *A*=0.004 and for (B) Canada Glacier *A*=0.004. The arrows show how the curve shifts from a to b to c when *C* is changed.

The inclusion of wind-speed (TIU-model) has a similar but opposite effect on predicted melt and stream flow volume as solar radiation in the TI-model. An increase in wind speed shifts the curve towards positive temperature reducing the modeled melt/stream flow with respect to temperature. When comparing the measured melt (half the total ablation) with respect to the estimated temperature at the stake locations for Howard and Taylor glaciers, melt on Howard Glacier occurs at cooler temperatures

than on Taylor (Figure 26). The average wind-speed is 4.5 ms^{-1} over Taylor Glacier and only 2.7 ms^{-1} over Howard Glacier. The same curve with D set to zero would overestimate melt for Taylor Glacier and underestimate melt for Howard Glacier.

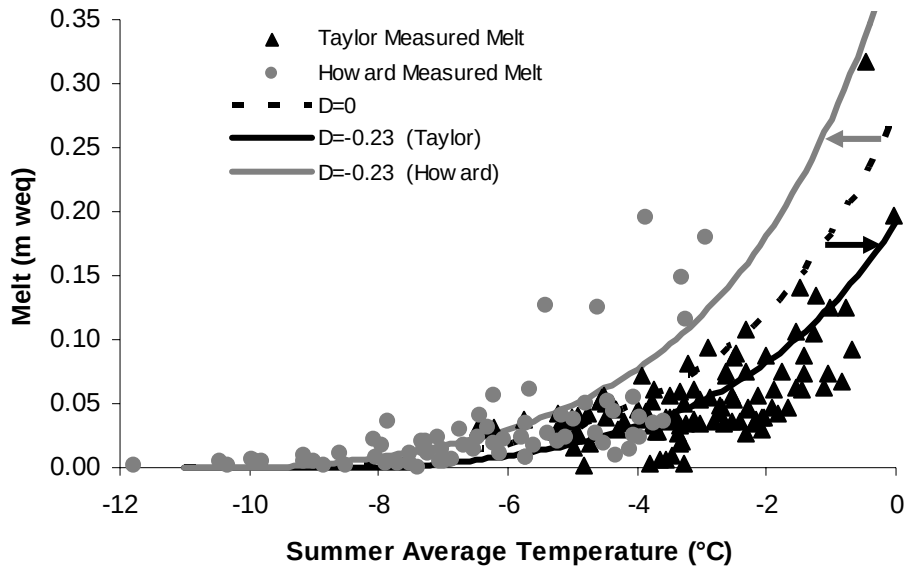

Figure 26: Effect of incorporating wind speed into the model for melt on Howard and Taylor glaciers. A=0.03, B=1.06, C=0

V RESULTS

The T-model was optimized using data from Canada and Commonwealth glaciers and applied to the rest of the glaciers. The TI-model was optimized using data from Howard, Canada and Commonwealth glaciers and the TIU-model was optimized using data from Taylor Glacier in addition to Howard, Canada and Commonwealth glaciers. The coefficients of the final models are presented in Table 6 and the values used to normalize the variables are presented in Table 7.

Table 6: Optimal coefficients for the temperature index model (T), the temperature-solar radiation model (TI) and the temperature-solar radiation-wind speed model (TIU).

Coefficients	T	TI	TIU
A	0.004	0.004	0.006
B	3.000	3.600	2.700
C	0.000	0.520	0.330
D	0.000	0.000	-0.176
E	-0.010	-0.010	-0.010

Table 7: Mean and standard deviation of variables used for normalization.

Variable	Mean	Standard Deviation
T	5.76	2.81
I	253.05	27.17
U	3.62	0.61

Melt/Ablation Results

To compare estimated melt with the ablation measurements of the stake networks on Canada, Commonwealth, Howard and Taylor Glaciers, summer average temperature (equation 9) and then melt (equations 17-19) was calculated at each stake for each season (Figure 27). For Canada and Commonwealth glaciers, the T-model closely matches the half-ablation and is in most cases below the measured ablation.

The predicted melt for Howard Glacier is below the half-ablation group, and the predicted melt for Taylor Glacier is well above the total ablation.

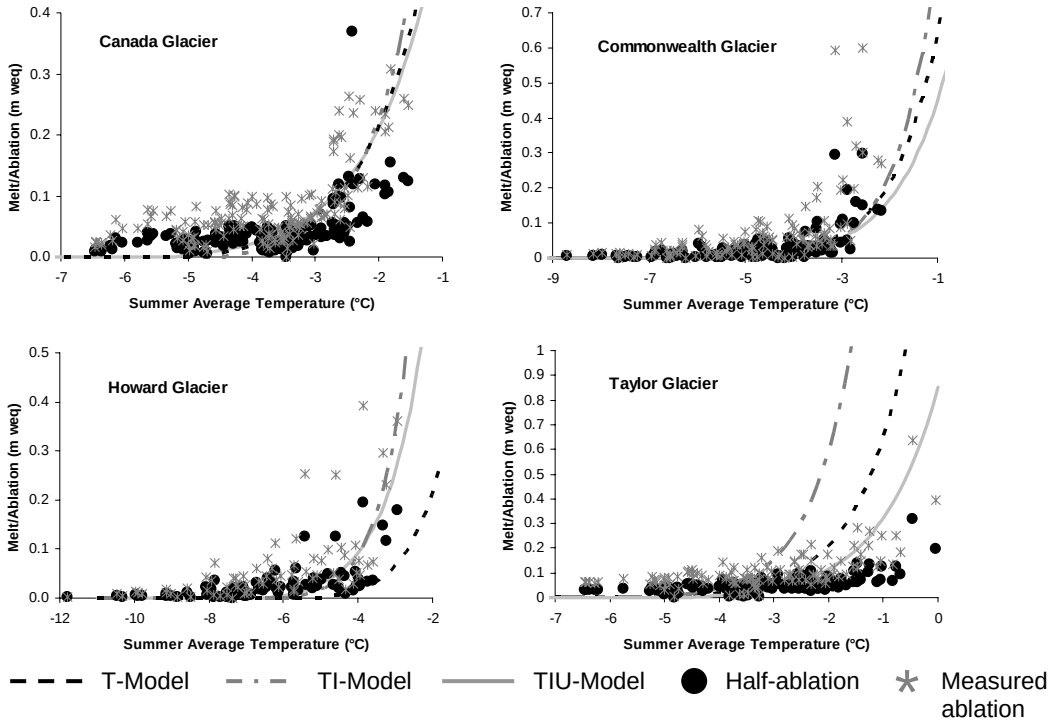

Figure 27: Comparison of modeled melt and measured ablation for Canada, Commonwealth, Howard and Taylor glaciers. Summer average temperatures were calculated at each stake from equation (9).

The large underestimate of melt on Howard Glacier in the Kukri Hills is due, in part, to the fact that Howard Glacier slopes towards the north. The sun is higher in the northern sky (36° above horizontal at solstice) compared to the southern sky (10.5° above horizontal at solstice) resulting in a significant difference in potential solar radiation (roughly 266 and 242 Wm^{-2}) on the glacier surfaces in the Kukri Hills and the Asgard Range, respectively.

To better account for spatial differences in solar radiation, the TI-model was applied. Melt estimates for Canada and Commonwealth were similar to those from

the T-model (Figure 27). The results for Howard Glacier, however, significantly improved and closely followed the half-ablation values. Unfortunately, the melt at Taylor Glacier is overestimated, approximately 6 m (weq) of melt at a summer average temperature of -1 °C compared to measured ablation of less than 0.7 m (weq).

High average summer wind speeds and low humidity on Taylor Glacier may account for the large difference in predicted versus measured. Comparing wind speed and relative humidity on Taylor and Canada glaciers, for example, shows 4.5 ms^{-1} versus 3.2 ms^{-1} and 59% versus 65%, respectively. As previously mentioned, wind plays an important role in the energy balance. For air temperatures below freezing, common to summer air temperatures, higher winds enhance energy loss through latent and sensible heat exchange. Consequently, little energy is left over for melt. The TIU-model reduced the predicted melt for Taylor Glacier so that the melt curve at least lies within the measured ablation data. The modeled melt for Canada, Commonwealth and Howard glaciers again closely matches the half ablation and is in most cases below the measured ablation (Figure 27).

Stream Flow Volume Results

The accuracy of modeled stream flow is assessed by comparison with observed flows (Table 8). The statistical comparison is made both for individual streams and entire basins. Taylor Glacier is excluded from this analysis due to the poor quality of the observational data. These results demonstrate the ability of the model to predict stream flow volume from unmeasured glaciers and streams. The regression plots of

stream flow versus Lake Hoare summer average temperature for the basins, glaciers, and individual streams are shown in Figures 28, 29, and 30 respectively.

Table 8: Coefficients of determination and total volume difference for the temperature-index model (T), the temperature-solar radiation model (TI) and the temperature-solar radiation-wind speed model (TIU). The glacier name in italics follows the name of the stream that drains from it. Negative values of the coefficient of determination indicate the difference between the measured and calculated stream volume is greater than the variability of the measured stream flow volume. Negative values of total volume difference represent over predicted volume.

	Coefficient of Determination			Total Volume Difference (%)		
Contributing Area	**T-Model**	**TI-Model**	**TIU-Model**	**T-Model**	**TI-Model**	**TIU-Model**
Lake Fryxell Basin	0.60	0.73	0.67	27	15	13
Green Creek *Canada*	-0.06	-0.19	-0.28	-57	-54	-70
Canada Stream *Canada*	0.62	0.61	0.67	22	30	4
Lost Seal Creek *Commonwealth*	0.73	0.64	0.59	8	30	28
Aiken Creek *Commonwealth*	0.55	0.57	0.42	34	39	46
Commonwealth Stream *Commonwealth*	0.60	0.68	0.66	28	-2	12
Delta Stream *Howard*	-0.03	0.71	0.66	81	-25	-21
Crescent Stream *Crescent*	-0.43	0.24	0.51	99	-46	15
VonGuerard Stream *Unnamed*	-0.48	0.15	-0.20	100	73	90
Lake Hoare Basin	0.67	0.42	0.62	1	44	11
Andersen Creek *Canada*	0.66	0.59	0.65	-9	29	-5
House Stream *Suess*	0.48	-0.75	-0.01	35	95	65
Lake Bonney Basin	-0.19	-0.14	-0.97	63	63	84
Lawson Creek *Rhone*	-1.44	-3.60	-3.59	69	94	94
Priscu Stream *LaCroix, Sollas and Marr West*	0.17	0.59	-0.15	57	29	72
Canada Glacier	0.69	0.73	0.64	-9	6	-19
Commonwealth Glacier	0.67	0.73	0.61	22	21	27

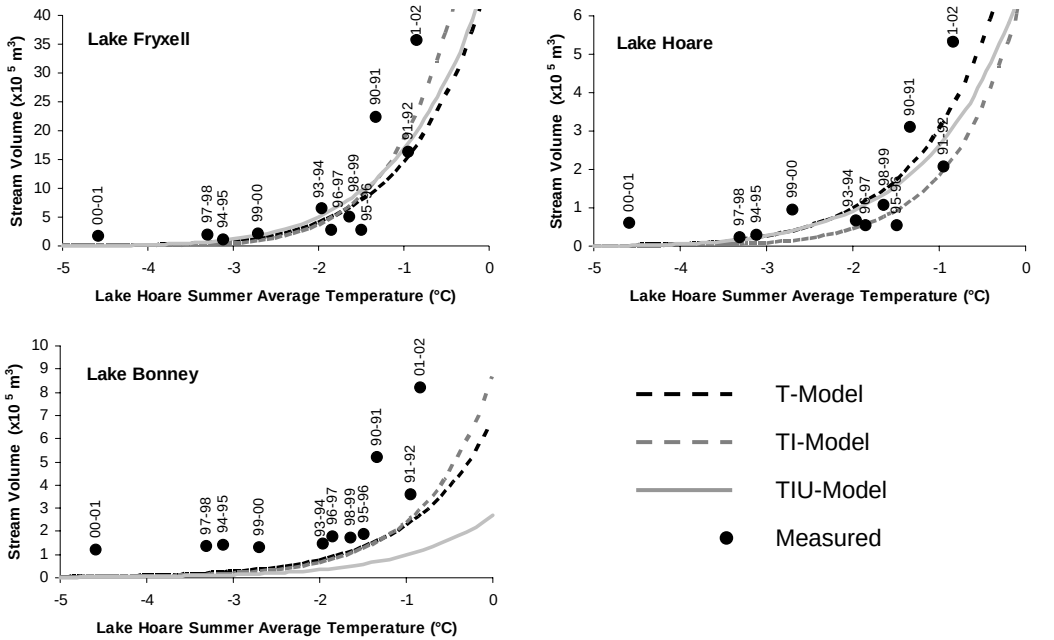

Figure 28: Modeled and measured stream volume into Lakes Fryxell, Hoare and Bonney.

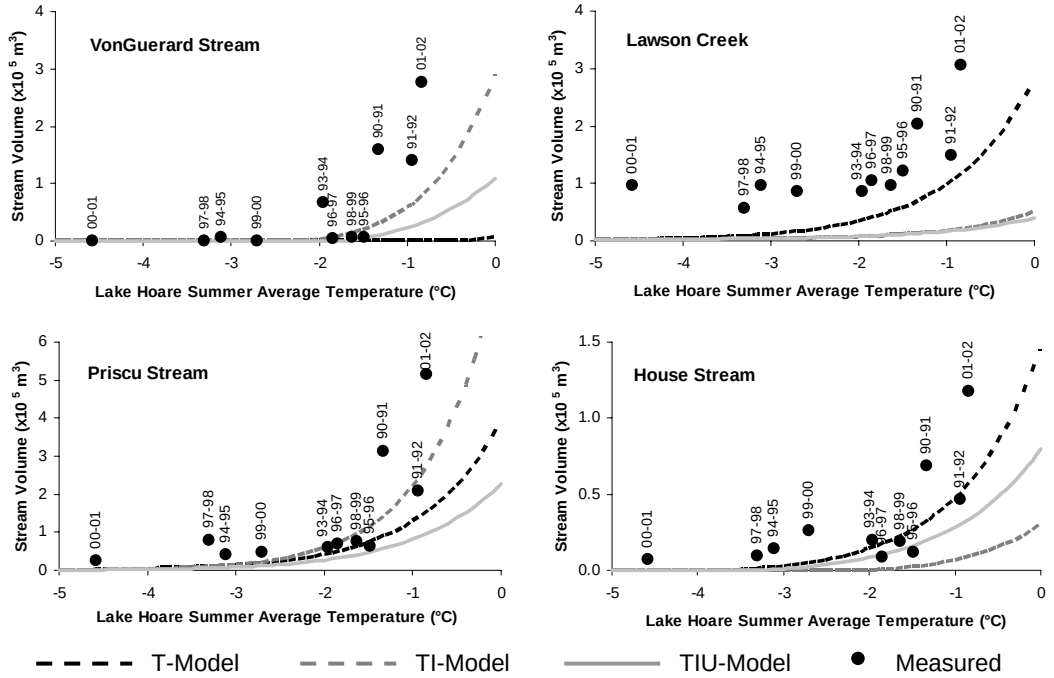

Figure 29: Modeled and measured stream volume for individual streams.

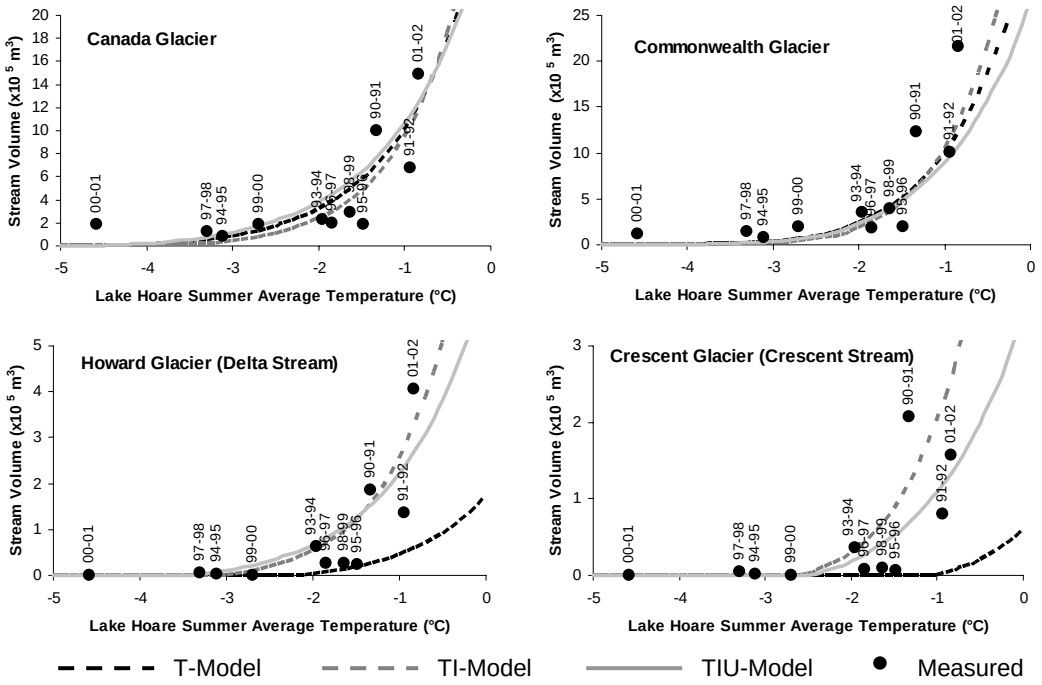

Figure 30: Modeled and measured stream volume for Canada, Commonwealth, Howard, and Crescent glaciers.

The T-Model performed well in the Lake Fryxell and Lake Hoare basins with r^2 values of 0.60 and 0.67 respectively. The model underestimates the total stream flow volume for the eleven seasons by 27% for the Fryxell Basin and by only 1% for the Hoare Basin. The model performs poorly in the Bonney Basin, underestimating total stream flow volume for Lawson and Priscu streams over the eleven seasons by 63%. In the Lake Fryxell Basin, the model performs well for four of the five streams draining from south-facing Canada and Commonwealth glaciers (Table 8). Total stream flow from Green Creek, where the model performs poorly, is overestimated by 57%. This may be a result of overestimation of the contributing area for Green Creek (Figure 18) since stream flow volume is underestimated for the other three streams. In contrast, stream flow volume is underestimated by 80% to 100% for the streams,

Delta, Crescent and VonGuerard, all of which drain from the north-facing glaciers of the Kukri Hills. Two streams flow to Lake Hoare, Andersen Creek from Canada Glacier and House Stream from Suess Glacier. The T-Model performed well for these streams, overestimating total stream flow for Andersen Creek by 9% and underestimating stream flow volume for House Stream by 35%. Stream flows into Lake Bonney—Lawson Creek from Rhone Glacier and Priscu Stream from LaCroix, Sollas and Marr West glaciers—are underestimated by 69% and 57% respectively.

The TI-Model improved the results for the north-facing glaciers in the Kukri Hills with little change in the results from the south-facing Canada and Commonwealth glaciers. The r^2 value for the Fryxell Basin increased to 0.73 and the total stream flow volume error was reduced to 15%. The reduction in error is largely from the increased calculated stream flow volume for Delta, Crescent and VonGuerard streams from the solar radiation term. The r^2 value for Delta Stream jumped to 0.71 and the values for Crescent and VonGuerard streams increased to 0.24 and 0.15 respectively. The total stream flow volume for Delta and Crescent streams are overestimated by 25% and 46% respectively and that for VonGuerard Stream is underestimated by 73%. Some of the water in VonGuerard Stream comes from a tributary stream from Crescent Glacier (Figure 1). It is unknown how much of VonGuerard's total stream flow volume comes from this tributary stream but this may account for some of the error. Statistics for the stream flow from Crescent and VonGuerard Streams combined show a smaller 21% error in total volume.

The TI-Model did not improve results in the Lake Hoare Basin. The r^2 value for Lake Hoare decreased from 0.67 to 0.42 and the total volume is underestimated by 44%. Most of this error is from decreased estimates of House Stream flow (95%). Decreased flow is caused by below average solar radiation, 214 Wm^{-2} compared to 253 Wm^{-2}. Considering that most of the stream flow into Lake Hoare comes directly from Canada Glacier, the effect of the under-predicting Suess on the total water input to the lake is small. Severe under prediction also occurs for Lawson Creek in the Bonney Basin. The total volume difference for Lawson increased from a 69% underestimate from the T-model to a 94% underestimate from the TI-model. Solar radiation is relatively low for Rhone, Suess and La Croix glaciers (Table 5) because they have steep south facing slopes. For example, the solar radiation value for Rhone is only 210 Wm^{-2}. The low solar radiation values on these glaciers cause the TI-model to under predict their melt and stream volume.

The TIU-model performed well in the Fryxell and Hoare basins. Results for the TIU model were similar to those of the TI-model in the Fryxell Basin with an r^2 of 0.67 and 13% underestimate in total stream volume. The results changed little for the individual streams in the Fryxell Basin except for Crescent Stream where r^2 jumped from 0.24 with the TI-model to 0.51 with the TIU-model. Results in the Hoare Basin improved over the TI-model with an r^2 of 0.62 due to an increased stream flow volume for both streams. In the Lake Bonney Basin, the total stream volume for Lawson and Priscu streams are severely underestimated (94% and 72% respectively) because the higher wind speeds in the Bonney Basin reduce the modeled stream volume for these

streams. Unfortunately, the ability of these models to predict total stream volume into the Bonney Basin cannot be sufficiently examined in any detail because of the lack of good quality stream data from the largest contributor to the lake, Taylor Glacier.

The streams in the valley are unequal in their importance to the total input into the lakes. For example, Canada Stream is generally the largest contributor to Lake Fryxell, Lost Seal is the second largest, and Crescent, VonGuerard and Huey streams are generally the smallest contributors to Lake Fryxell. The total volume from the three small contributors combined is almost always smaller than the volume of one of the large contributors alone. Therefore it is more important to get good results from the large contributors than from the small. Fortunately, the models performed their best for the large magnitude streams of Canada, Lost Seal, Aiken and Commonwealth in the Fryxell basin and Andersen in the Hoare basin. The models performed poorly for the large streams, Green Creek in the Fryxell Basin and Lawson and Priscu streams in the Bonney Basin.

Threshold Temperature and Melt Limit Results

The melt threshold temperature, the summer average temperature below which no melt is predicted (equation 24), for the T-model is -4.9°C throughout the valley (Table 9). This is comparable to Johnston's (2004) threshold (-4.4°C) for the onset of rapid channel growth on Taylor Glacier. The melt threshold temperature represents the minimum summer average temperature required for seasonal melt to occur. This does not mean that melt actually occurs at the threshold temperature. Figure 31 shows the melt limits and estimated equilibrium line altitudes (ELAs) for six glaciers in

Taylor Valley. The ELAs were estimated from the elevation where the glacier surface transitions from a convex (ablation zone) to a concave (accumulation zone) surface morphology (Leonard and Fountain, 2003), which were estimated on USGS topographic maps (Fountain and others, 1999a). The melt limits for Canada and Commonwealth glaciers hover around their ELAs (375 m), with averages of 390 m and 370 m respectively. However, the melt limits for Howard, Crescent and VonGuerard glaciers barely reach their ELAs during the warm seasons and are well below their ELAs during the cold seasons. The melt limit for Rhone Glacier is well below the ELA for all seasons.

Table 9: Threshold temperatures in °C and average melt limits and ELA in m above seal level for each glacier and model.

	Threshold Temp			Melt Limit			ELA
Glacier	T	TI	TIU	T	TI	TIU	
Canada	-4.9	-4.5	-5.4	394	341	449	375
Commonwealth	-4.9	-4.5	-5.0	372	313	390	375
Howard	-4.9	-5.7	-6.4	437	540	621	500
Crescent	-4.9	-6.2	-6.5	440	588	617	500
VonGuerard	-4.9	-6.4	-6.4	440	610	613	450
Rhone	-4.9	-2.7	-3.2	550	313	365	1000
Average	-4.9	-5.0	-5.5	439	451	509	533

The solar radiation term in the TI-model lowered the threshold temperatures for Howard, Crescent, and VonGuerard glaciers. Lower threshold temperatures increase the melt water flux at any point previously contributing, increase the elevations of the melt limits and therefore increase the contributing area. The melt limits increased for all three glaciers in the Kukri Hills by ~150m from the T-model to the TI-model. The threshold temperature for both Canada and Commonwealth

glaciers increased to -4.5°C with the TI-model producing melt limits ~60 m lower than those from the T-model. The low solar radiation of Rhone Glacier increased the threshold temperature by +2.2°C to -2.7°C from the T-model which requires warmer temperatures for melt to occur. The melt limits of Rhone for the TI-model are ~240 m lower than those from the T-model leaving even less contributing area for melt. For the TIU-model, Taylor and Rhone have the warmest threshold temperatures and Howard, Crescent and VonGuerard have the coldest. As a result, Taylor and Rhone have the lowest estimated melt rate where Howard, Crescent and VonGuerard have the highest. This improved the melt prediction for Taylor Glacier but made no improvement for Rhone.

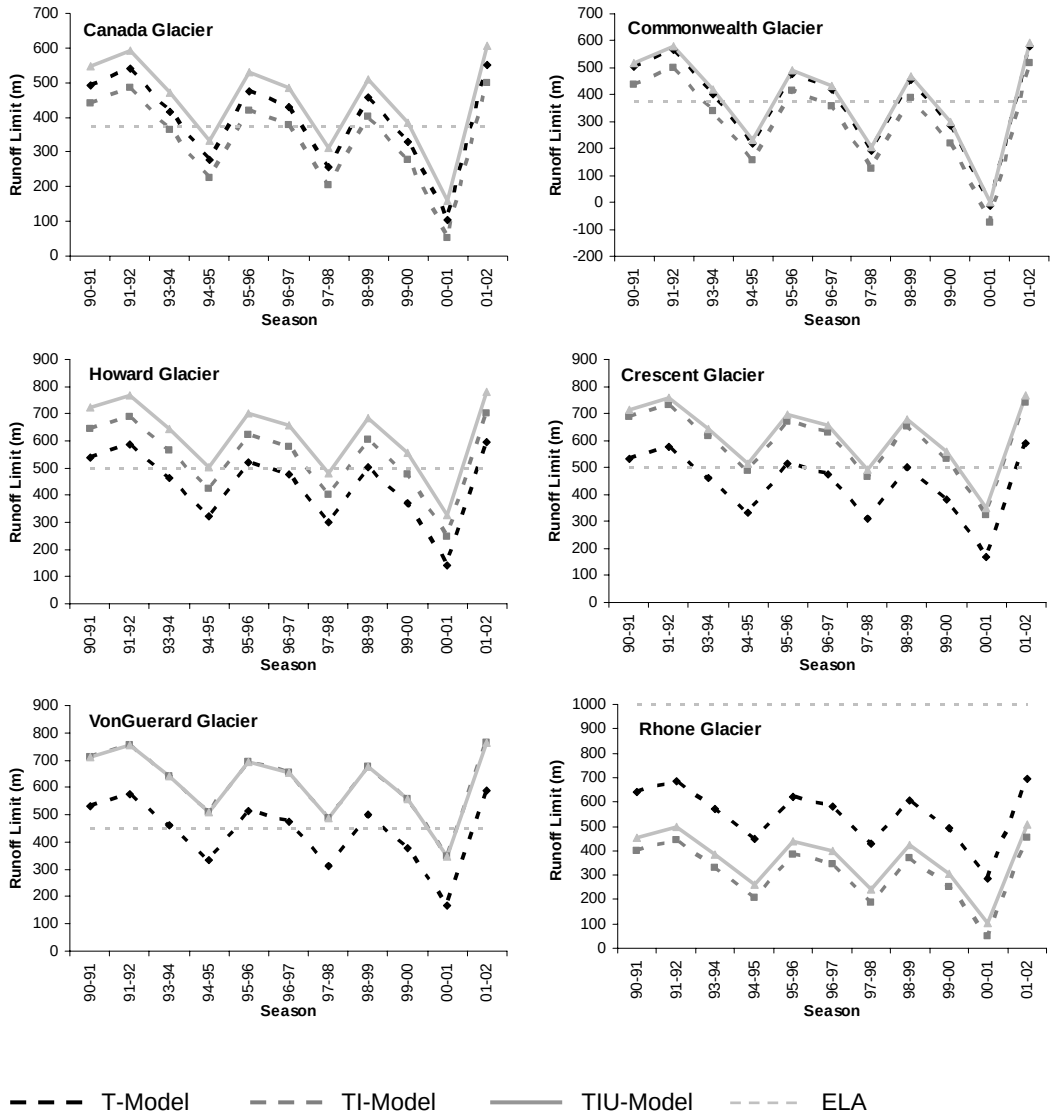

Figure 31: Melt limit and ELA for Canada, Commonwealth, Howard, Crescent, VonGuerard and Rhone glaciers.

VI ERROR ANALYSIS

There are two types of errors inherent in these models—spatial, in which the models will yield poor results for some glaciers while yielding good results for others and temporal in which the models perform well for some years and poorly for others. For the spatial errors, the largest occurred at Rhone, Suess, and LaCroix glaciers where all three models underestimate stream volume and at Taylor Glacier where the T and TI-models overestimate melt. Rhone, Suess, and LaCroix glaciers are characterized by steep rough surfaces with many vertical walls, which enhance surface melt. Vertical walls enhance solar intensity when the sun is low in the sky, and reduce wind speed, which reduces the turbulent heat losses and leaves more energy available for melt (Lewis and others, 1999; Johnston and others, in press). On Suess Glacier, rock debris spread over the surface also enhances melt. I believe that the different surface roughnesses of these glaciers are responsible for their different melt behavior. Taylor Glacier is characterized by a smooth flat surface with melt channels incised into the surface near the terminus. High wind speeds and low humidity over Taylor Glacier favor sublimation over melt. The T-model and TI-model overestimate melt for this glacier, whereas the TIU-model improved the result for only Taylor.

A second source of spatial error is calculated temperatures from equation (10) (Figure 14). The melt models depend on these calculated temperatures and thus inherit their errors. The standard deviation of the residuals between measured and calculated temperatures at the seven meteorological stations in the valley is 0.36°C. To test the effect of errors in calculated temperature on modeled melt, three melt

curves were plotted together one with the estimated temperatures, one with a + 0.36°C shift and one with a – 0.36°C shift (Figure 32). This provides a maximum range of melt and stream volume values. Because of the nature of the exponential equation, the modeled melt and stream volume is most sensitive to errors in estimated temperatures at warmer temperatures.

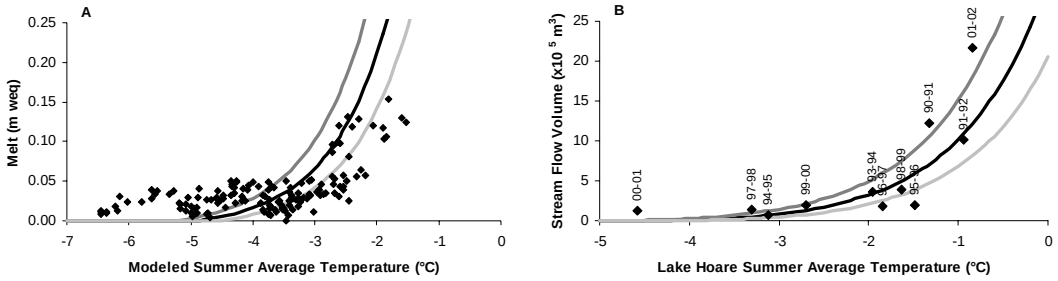

Figure 32: Effect of errors in temperature for melt (A) and stream flow volume (B) from Canada Glacier. The points are measured melt (half ablation) in A and measured stream flow volume in B.

The temporal errors are, in part, a result of a poor fit to the data for some temperature ranges and a result of scatter in the data (Figure 33 and 34). The residuals were normalized by dividing them by the measured stream flow volume to better compare differences between modeled and measured. The residuals in the Bonney Basin show large underestimations of stream flow for all seasons because of the poor performance of the models for Lawson and Priscu streams. Many of the residuals result because some relatively cool seasons (1993-1994, 1998-1999) produced more stream flow volume than some warmer seasons (1996-1997, 1995-1996). Also the model underpredicts flow at low temperatures (Figure 35).

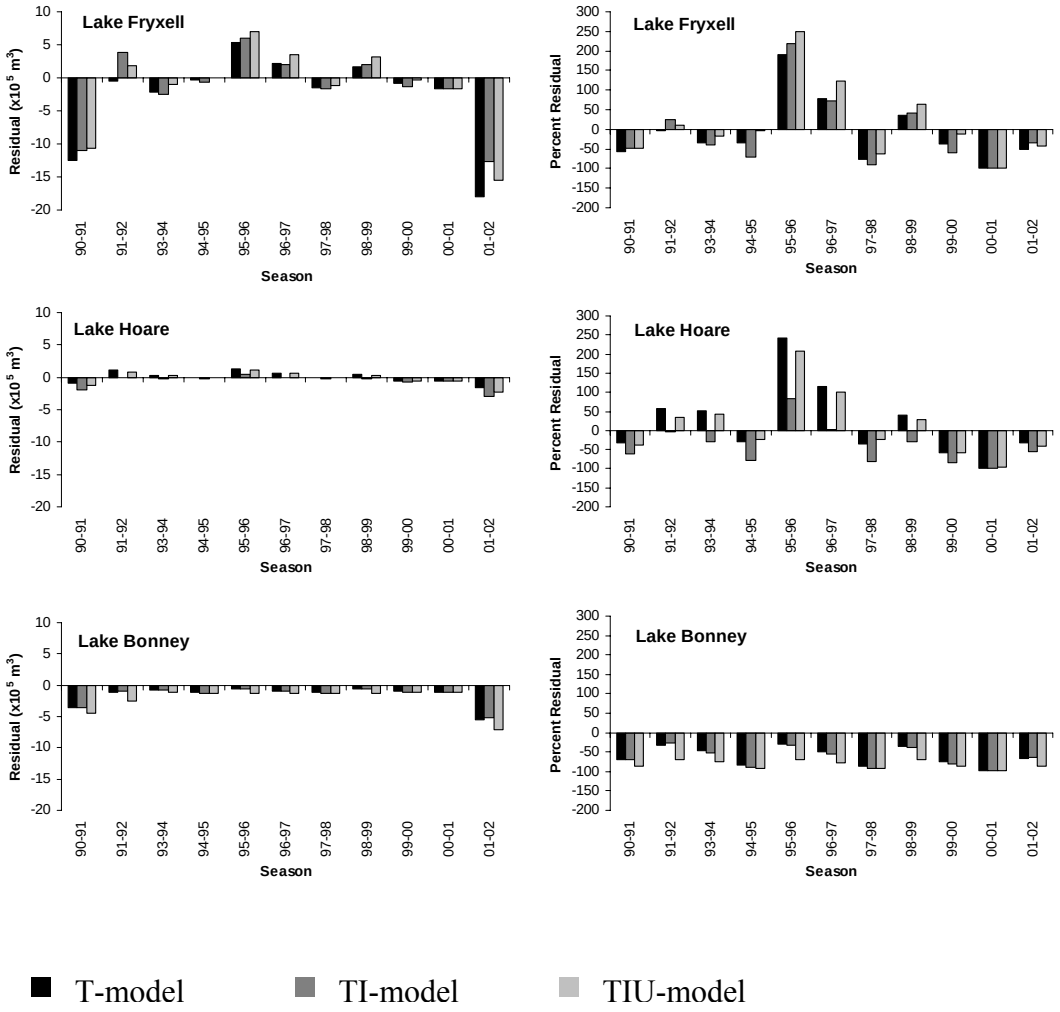

Figure 33: Lake Fryxell, Hoare and Bonney basin residuals. The left hand column is the residual (modeled minus measured stream flow volume) and the right hand column is the normalized residual (residual divided by measured stream flow volume) shown here as a percentage.

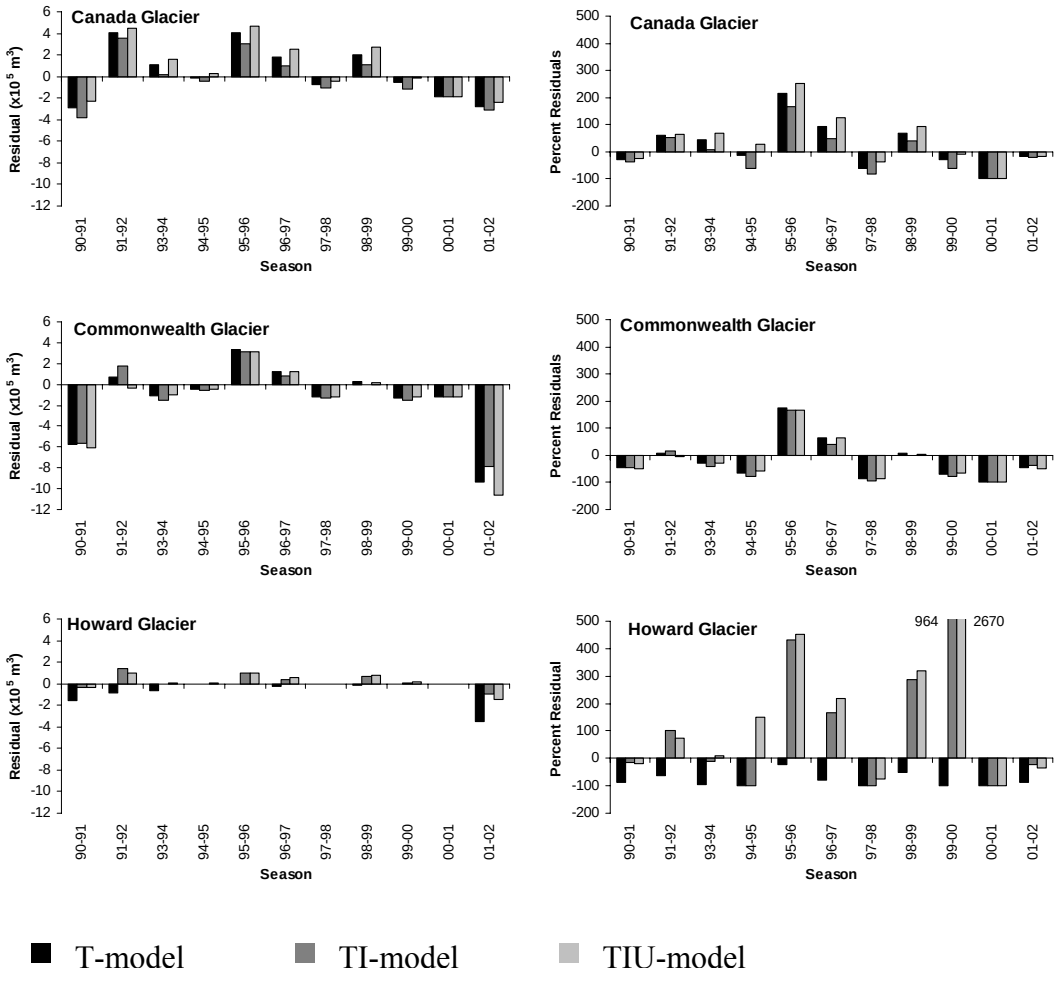

Figure 34 Canada, Commonwealth and Howard glacier residuals. The left hand column is the actual residual (modeled minus measured stream flow volume) and the right hand column is the normalized residual (residual divided by measured stream flow volume) shown here as a percentage.

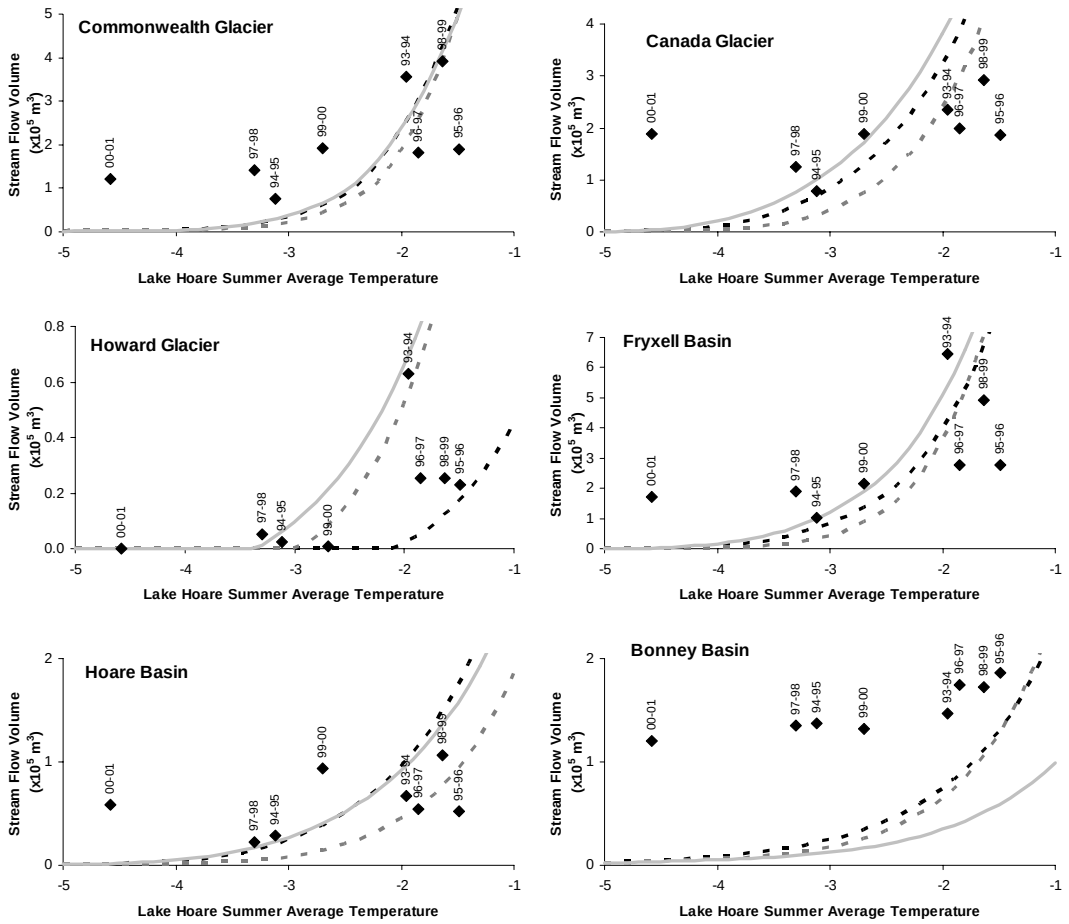

Figure 35: Replot of Figure 28 and 30 to highlight the model underestimate in the colder, low flow seasons.

To examine why some relatively cool seasons produced more stream flow volume than some warmer seasons, I examine air temperature and the other meteorological values that affect the energy balance. I first compare degree-days because the models use summer average temperature to calculate melt rather than the span of time the temperatures were above the melting temperature. This difference could lead to an over or underestimation of modeled melt. For example, the 1990-1991 season had a colder temperature (-1.33°C) than the 1991-1992 season (-0.94°C)

but yielded more stream flow. The 1990-1991 season had an intense cold period early in the season but warmer temperatures in mid season than the 1991-1992 season. Most of the melt is generated in mid season.

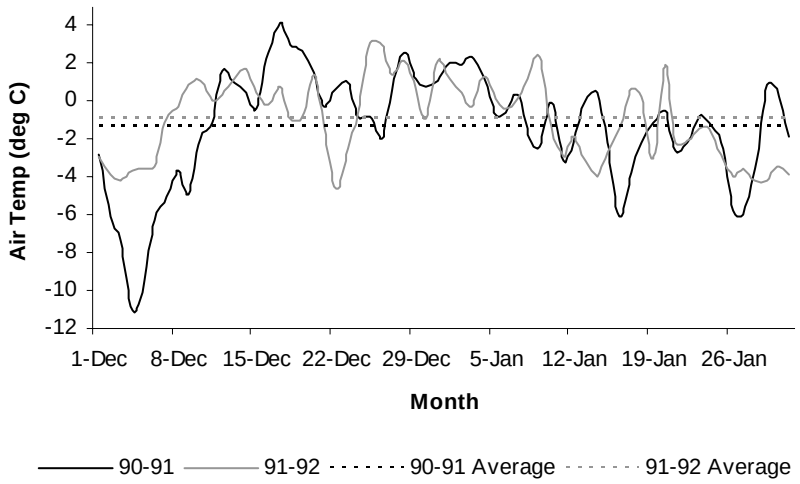

Figure 36: 1990-1991 and 1991-1992 Lake Hoare daily average temperatures.

The calculation of degree-days in equation (4) sums the temperatures above a threshold temperature and may provide a more sensitive indicator of melt than average temperature. The number of degree-days for each season at Lake Hoare was calculated using 0ºC and -4.9ºC threshold temperatures (the latter being the threshold temperature for the T-model (Table 9)) and the 10-minute to 6-hour temperature data, depending on the data collection intervals, from December 1 to January 31. Lake Hoare summer average temperatures and degree-days are presented in Table 10, then normalized and plotted in Figure 37. Degree-days with -4.9ºC threshold temperature follow the average temperature more closely than degree-days with -0ºC threshold temperature.

Table 10: Lake Hoare summer average temperature and degree-days.

Season	Average Temperature (°C)	Degree-Days (°C-day) (T_0=0°C)	Degree-Days (°C-day) (T_0=-4.9°C)	Stream Flow Volume ($x10^5$ m^3) Fryxell	Hoare	Bonney
90-91	-1.33	39.06	243.43	22.4	3.1	5.2
91-92	-0.94	36.52	246.66	16.2	2.1	3.6
93-94	-1.96	8.36	126.68	6.4	0.7	1.5
94-95	-3.12	2.39	97.13	1.0	0.3	1.4
95-96	-1.49	24.47	213.76	2.7	0.5	1.9
96-97	-1.85	15.57	196.04	2.8	0.5	1.7
97-98	-3.30	10.57	133.02	1.9	0.2	1.4
98-99	-1.63	24.52	212.11	4.9	1.1	1.7
99-00	-2.70	2.82	150.04	2.2	0.9	1.3
00-01	-4.58	0.26	67.27	1.7	0.6	1.2
01-02	-0.84	57.23	259.16	33.4	5.3	8.2
Average	-2.14	20.16	176.66	8.7	1.4	2.6
Standard Deviation	1.15	18.7	62.22	10.7	1.6	2.2

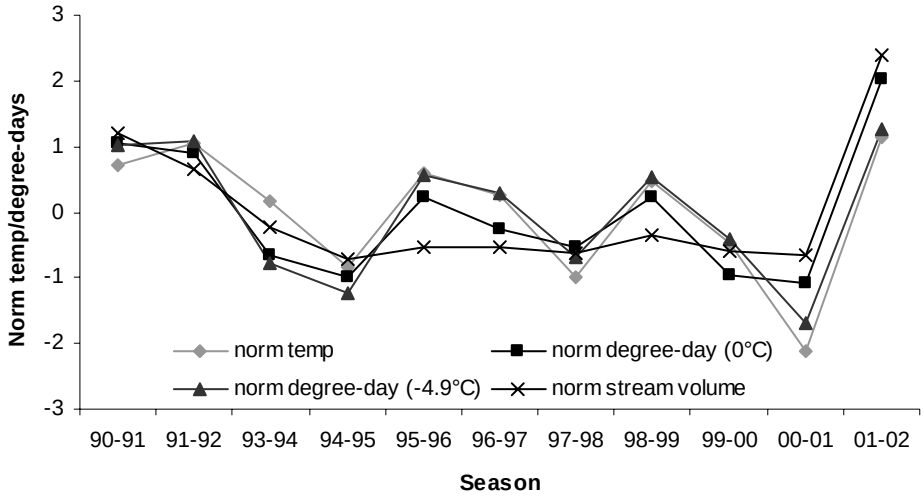

Figure 37: Lake Hoare normalized average temperature and degree-days.

I expect the seasons where the normalized degree-day is larger than the normalized average temperature to be those with relatively high stream volumes during relatively cold temperatures and vice-versa. Comparisons of the difference

between normalized air temperature and normalized stream flow volume and the difference between the normalized air temperatures and the normalized degree-days (Figure 38) shows that this is the case for most seasons.

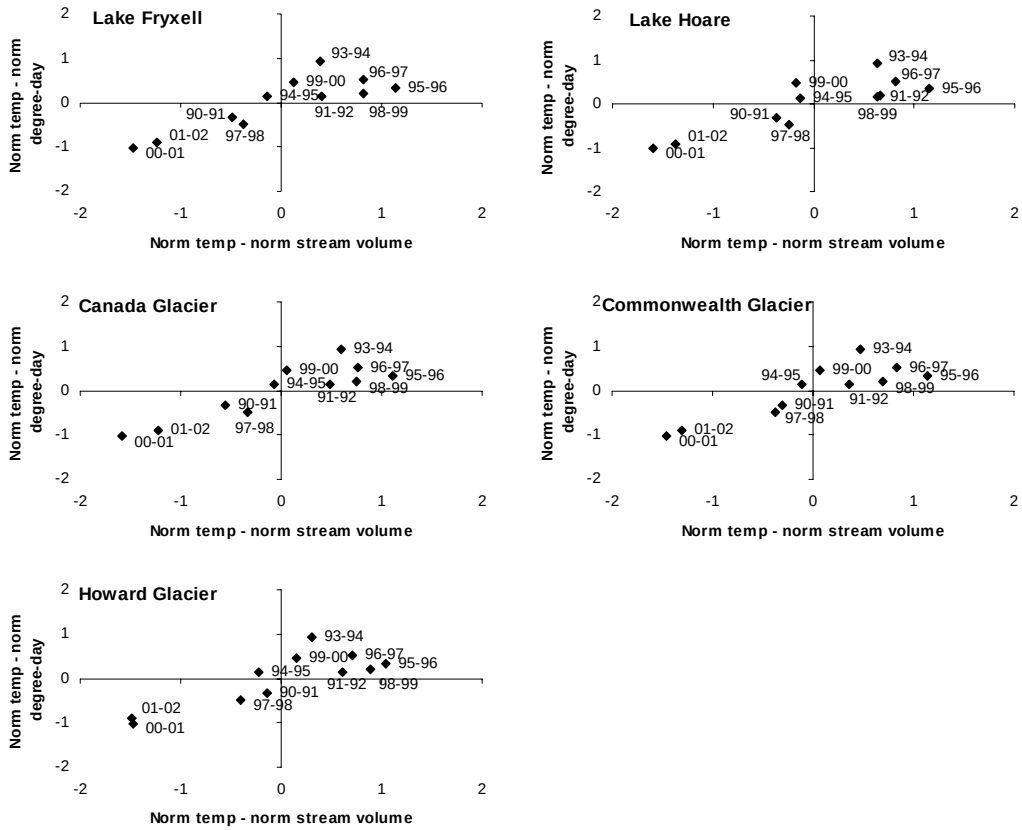

Figure 38: Normalized Lake Hoare air temperature minus normalized stream volume from Lake Fryxell, Lake Hoare, Canada Glacier, Commonwealth Glacier and Howard Glacier versus the difference between Lake Hoare normalized air temperature and Lake Hoare normalized degree-days.

For the case of the 1990-1991 and 1991-1992 seasons mentioned earlier, the 1990-1991 season, which had 1.5 times more stream flow than 1991-1992, had more degree-days (39) than the 1991-1992 season (36.5). An extreme case is the 2001-2002 season, which experienced more than double the stream flow than the 1991-1992

season, which was only 0.1°C cooler. The difference in stream flow here can also be explained by degree-days, 2001-2002 had 57 and 1991-1992 had 36.5. As shown in Figure 38, degree-days/average temperature help explain the scatter in the stream volume-temperature relationship for all seasons except 1994-1995.

The residuals may also be examined by comparison with meteorological data (summer average relative humidity, wind speed, shortwave radiation, and albedo) (Figure 39). I normalized the meteorological data using equation (21) and compared them with the difference between normalized air temperature and normalized measured stream volume (Figure 40-44).

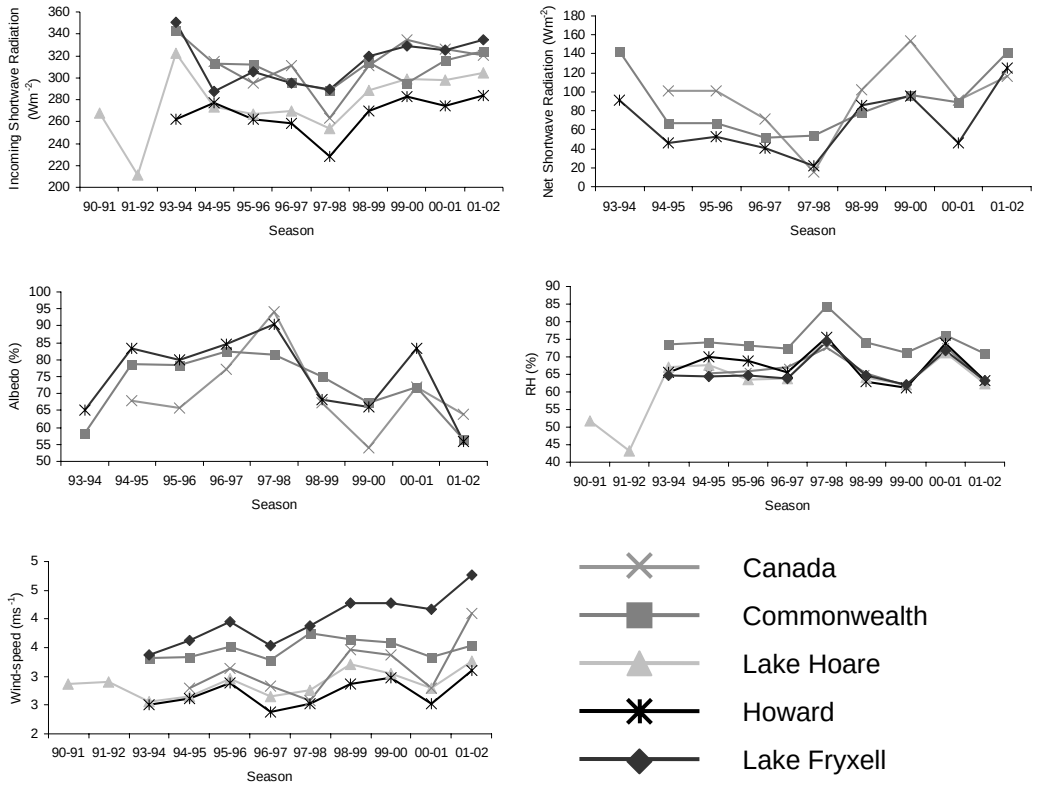

Figure 39: Summer average meteorological data from Lake Hoare, Lake Fryxell, Commonwealth Glacier, Canada Glacier and Howard Glacier.

High relative humidity favors melt compared to sublimation via the latent heat term in the energy balance. Figure 40 shows that high relative humidity in 1997-1998 and 2000-2001, and low relative humidity in 1991-1992 may account for the difference between temperature and stream volume.

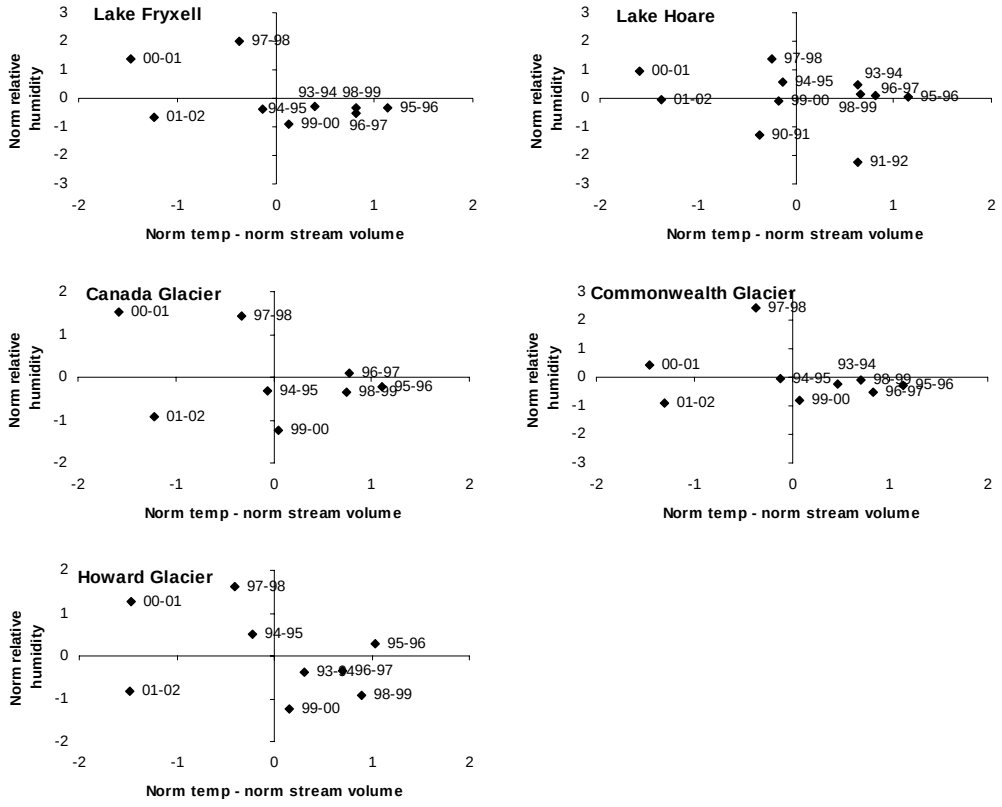

Figure 40: Normalized air temperature minus normalized stream volume versus normalized relative humidity for Lakes Fryxell and Hoare, and Canada, Commonwealth and Howard Glaciers.

High wind-speed favors sublimation through the latent heat term in the energy balance leaving less energy for melt. Figure 41 shows that low wind-speed may account for relatively high stream flow in 1990-1991, 1994-1995, 1997-1998, and 2000-2001 and high wind-speed may account for relatively low stream flow in 1995-1996, 1998-1999 and 1999-2000.

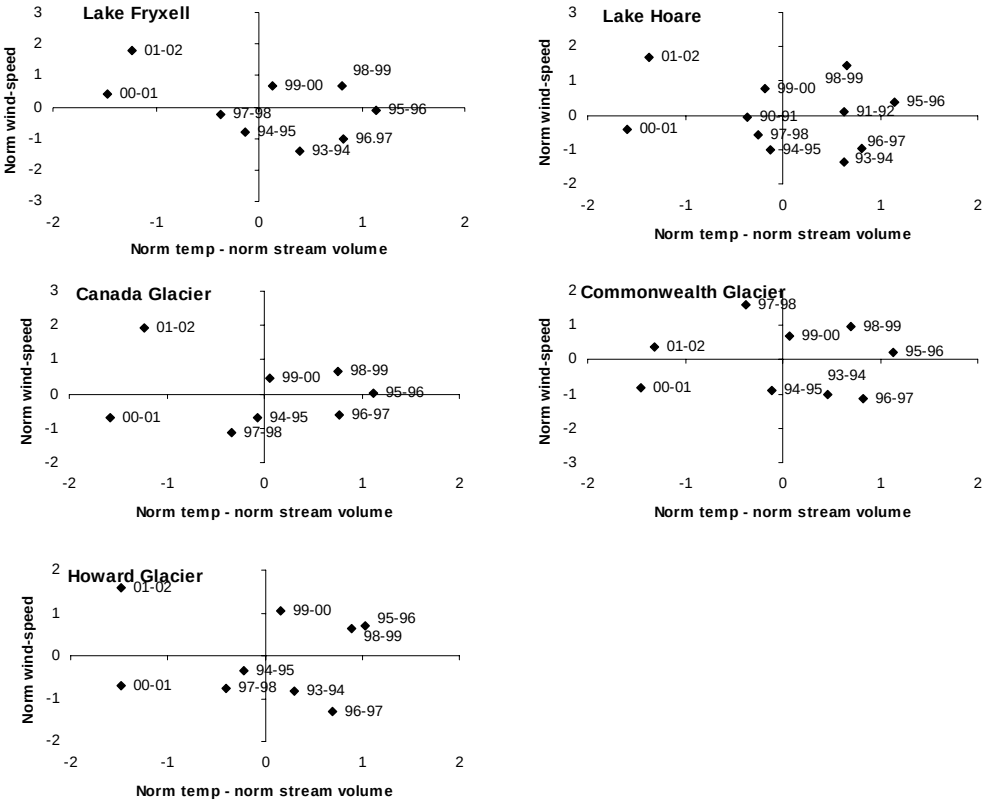

Figure 41: Normalized air temperature minus normalized stream volume versus normalized wind-speed for Lakes Fryxell and Hoare, and Canada, Commonwealth and Howard Glaciers.

Incoming short-wave radiation depends on the atmospheric conditions including cloud cover and atmosphere transparency. Relatively high incoming short-wave radiation indicates clear days, enhancing heating of the ice and melting. The plots in Figure 42 show that relatively high stream flow in 2000-2001 and 2001-2002 can be accounted for by relatively high incoming shortwave radiation and low stream flow in 1991-1992, 1995-1996, and 1996-1997 can be accounted for by low incoming shortwave radiation.

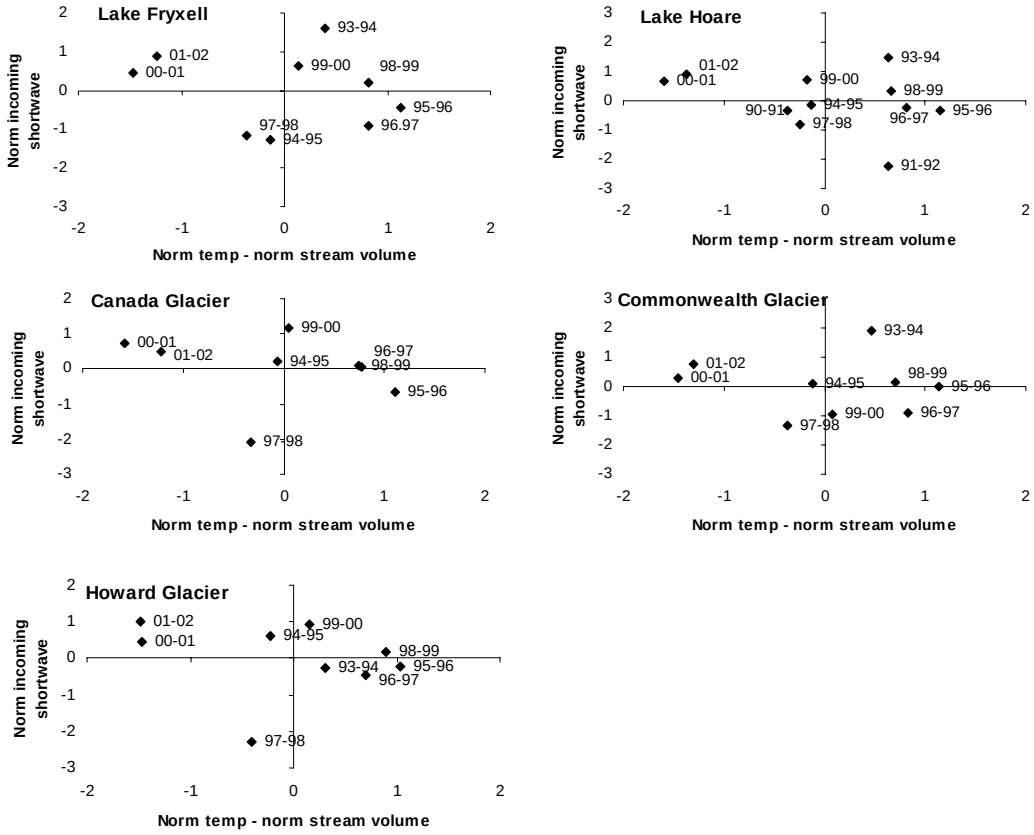

Figure 42: Normalized air temperature minus normalized stream volume versus normalized incoming shortwave radiation for Lakes Fryxell and Hoare, and Canada, Commonwealth and Howard Glaciers.

Glaciers with high albedo will melt less than glaciers with low albedo. Albedo, the fraction of incoming shortwave-radiation reflected by the surface, increases with the presence of snow on the glacier surface and the presence of ice or sediment decreases the albedo. The plots in Figure 43 shows that low albedo in 2001-2002 and high albedo in 1995-1996, 1996-1997, and 1998-1999 may account for the difference between temperature and stream volume.

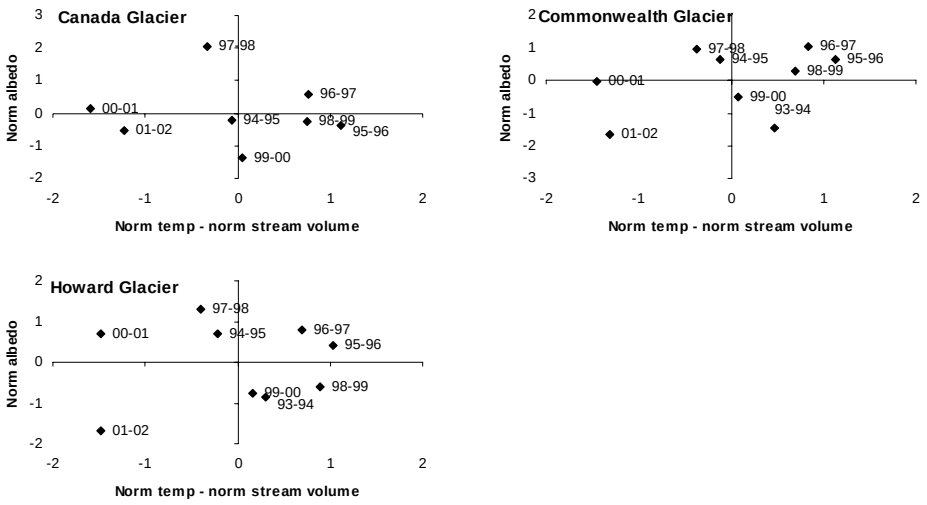

Figure 43: Normalized air temperature minus normalized stream volume versus normalized albedo for Canada, Commonwealth and Howard Glaciers.

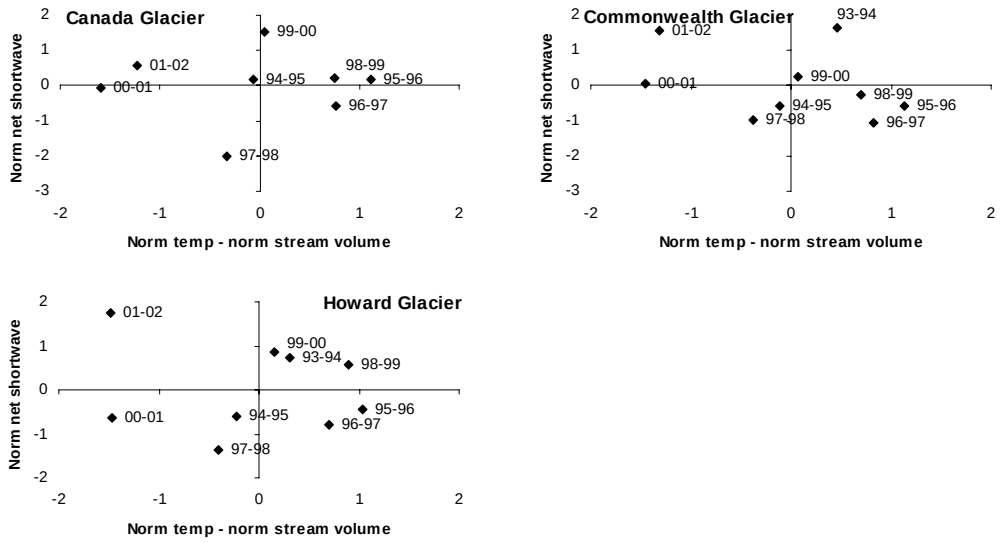

Figure 44: Normalized air temperature minus normalized stream volume versus normalized net shortwave radiation for Canada, Commonwealth and Howard Glaciers.

High net shortwave radiation enhances melt. The net shortwave radiation is the magnitude of radiation that is absorbed by the surface (incoming minus outgoing). This is dependent on both the incoming short-wave radiation and the albedo. As with albedo, high net shortwave radiation in 2001-2002 and low net shortwave radiation in

1995-1996, 1996-1997 and 1998-1999 may explain the difference between temperature and stream volume (Figure 44).

In summary, Table 11 and 12 show the seasons in which degree-days and the meteorological data may qualitatively explain the scatter between air temperature and measured stream volume. Of all of the variables involved in the stream flow estimation, degree-days can explain most of the scatter followed by net radiation and relative humidity.

Table 11: Summary of seasons where degree-days and meteorological data explain the scatter between air temperature and measured stream volume where stream volume is high and temperature low.

	Season	High D-days	High RH	Low Wind-speed	High SW In	Low Albedo	High Net SW
Lake Hoare	90-91	X		X		n/a	n/a
	94-95		X	X		n/a	n/a
	97-98	X	X	X		n/a	n/a
	99-00				X	n/a	n/a
	00-01	X	X	X	X	n/a	n/a
	01-02	X			X	n/a	n/a
Lake Fryxell	90-91	X				n/a	n/a
	94-95			X		n/a	n/a
	97-98	X	X	X		n/a	n/a
	00-01	X	X		X	n/a	n/a
	01-02	X			X	n/a	n/a
Canada Glacier	90-91	X					
	94-95			X	X	X	X
	97-98	X	X	X			
	00-01	X	X	X	X		
	01-02	X			X	X	X
Commonwealth Glacier	90-91	X					
	94-95			X	X		
	97-98	X	X				
	00-01	X	X	X	X	X	X
	01-02	X			X	X	X
Howard Glacier	90-91	X					
	94-95		X	X	X		
	97-98	X	X	X			
	00-01	X	X	X	X		
	01-02	X			X	X	X

Table 12: Summary of seasons where degree-days and meteorological data explain the scatter between air temperature and measured stream volume where stream volume is low and temperature high.

	Season	Low D-days	Low RH	High Wind-speed	Low SW In	High Albedo	Low Net SW
Lake Hoare	91-92	X	X	X	X	n/a	n/a
	93-94	X				n/a	n/a
	95-96	X			X	n/a	n/a
	96-97	X			X	n/a	n/a
	98-99	X		X		n/a	n/a
Lake Fryxell	91-92	X				n/a	n/a
	93-94	X	X			n/a	n/a
	95-96	X	X	X	X	n/a	n/a
	96-97	X	X		X	n/a	n/a
	98-99	X	X			n/a	n/a
	99-00	X	X	X		n/a	n/a
Canada Glacier	91-92	X					
	93-94	X					
	95-96	X	X	X	X		
	96-97	X				X	X
	98-99	X	X	X			
	99-00	X	X	X			
Commonwealth Glacier	91-92	X					
	93-94	X					
	95-96	X	X	X		X	X
	96-97	X	X		X	X	X
	98-99	X	X	X		X	X
	99-00	X	X	X	X		
Howard Glacier	91-92	X					
	93-94	X	X		X		
	95-96	X		X	X	X	X
	96-97	X	X		X	X	X
	98-99	X	X	X			
	99-00	X	X	X			

VII DISCUSSION AND CONCLUSIONS

For this thesis, I developed a temperature-index model of stream flow across Taylor Valley that can be used to predict past stream flow when air temperature is the only available data. This work follows from Hock's (1999) work on Storglaciaren. By including spatial variations in potential direct solar radiation I found that incorporating potential direct solar radiation improved the melt prediction in the dry valleys. Many temperature index models are developed for hourly to daily time scales and use a degree-day model (Hock, 1999; Kane and Greck, 1997; Braithwaite, 1995; Kustas and Rango, 1994). My project differs by examining a seasonal scale, using average temperature.

In the MDV, this work has added to the work of Bomblies (1998) and Jaros (2003) who related glacier contributing area to stream flow. Bomblies (1998) weighted the contributing areas by topographic shading and found that the correlations between contributing areas and stream flow were barely significant. Jaros (2003) weighted the contributing areas by the air temperature decrease from the adiabatic lapse rate and found a significant correlation between stream flow and the contributing areas. I took this a step further and used this relationship to predict stream flow throughout the valley. Rather than correcting for topographic shading, I corrected for solar intensity determined by the glacier slope and aspect. The studies of Bomblies (1998) and Jaros (2003) were limited to the Fryxell Basin where I tried to extend the model into the rest of the valley. The problems I found with modeling stream flow in the Bonney Basin underscore the results of Fountain (1999b) and Johnston (2004) that

increased wind-speed in the Bonney Basin has a profound effect on the turbulent heat transfer favoring sublimation over melt (Fountain, 1999b) and conversely, surface roughness and debris cover on some of the glaciers in the Bonney Basin can increase their melt (Johnston, 2004).

The goal of this thesis was to develop a valley-wide temperature-index model of stream volume for Taylor Valley, Antarctica. I developed three models of summer stream flow volume for Taylor Valley, Antarctica based on summer average air temperature with spatial variations in potential solar radiation included in the second and third models and spatial variations in average wind speed included in the third model. Air temperature was interpolated across the valley with respect to elevation, distance from the coast and distance from the valley bottom by equation (10). The T-model worked well on Canada and Commonwealth glaciers because they have similar characteristics. It failed, however, to model the stream flow of glaciers with differing spatial characteristics simultaneously (e.g. Canada and Howard) or valley location (e.g. Canada and Taylor). The TI-model included spatial variations in potential solar radiation and was successful in modeling stream flow from the north and south facing glaciers of the Hoare and Fryxell basins. The TIU-model included spatial variations in summer average wind speed as well as potential solar radiation and was fairly successful in modeling the melt from Taylor Glacier as well as the stream flow from the glaciers of the Hoare and Fryxell basins. All three models performed poorly in modeling the stream flow from the steep, rough, south-facing glaciers Rhone, LaCroix, and Suess. Modeling results for these glaciers were poor partly due to large

differences in energy balance controls on the glaciers. In the Bonney Basin, it is difficult to develop a good model with little usable stream flow data. Overall, the best results come from the TI-model (equation 20) in the Fryxell Basin where A=0.004, B=3.6, C=0.52 and E=-0.01 (Table 6). These models also predict reasonable melt values compared to ablation measurements for Canada, Commonwealth and Howard glaciers. The good results for Canada, Commonwealth and Howard glaciers give me confidence in applying these models elsewhere. The melt limits for Canada, Commonwealth, Howard, Crescent and VonGuerard glaciers closely hover around their respective ELAs. For these glaciers, the TI-model can simulate spatial and temporal variations in the ELA. Finally, the TI-model predicts a spatial variation in melt threshold temperatures via differences in potential solar radiation, yielding melt at lower temperatures on the glaciers in the Kukri Hills (more radiation) than the Asgard Range (less radiation) (Table 8). The average seasonal threshold temperatures for the T, TI and TIU-models are below 0ºC (-4.9ºC, -5.0ºC and -5.5ºC respectively). These are comparable to Johnston's (2004) threshold (-4.4°C) for the onset of rapid channel growth on Taylor Glacier.

Errors in predicted stream flow volume result from errors in the spatial extrapolation or temporal variations in other climatic variables (e.g. net radiation, humidity) and surface morphologies that is not well resolved by the index models. Most temporal errors can be explained by degree-days and many can also be explained by a combination of meteorological variables including shortwave radiation, humidity, wind speed, and albedo.

There is room for much improvement on this model in the Bonney Basin. One possibility for improvement would be to add a factor for surface roughness and debris cover to improve the melt prediction for Rhone, LaCroix and Suess glaciers. Improvement in cliff melt may be important and attempts were made to incorporate cliff melt in the TI-model and TIU-model with no success. Although the cliffs receive very intense solar radiation for part of the day, resulting in melt, the rest of the day they are shadowed, so calculated daily averages yield solar radiation values lower than the surface. Perhaps if melt were calculated on a finer time scale (hourly) the high intensity of solar radiation when the cliffs are in the sun could be applied towards a larger flux of melt. Other factors that may be included to improve the prediction of cliff melt are increased long wave radiation from rock surfaces adjacent to the cliffs and reduced wind-speeds.

The TI-model can be applied to all of the glaciers in the three basins to predict the total water input to the lakes for any season in which air temperature data exists. This includes all seasons with air temperature data from McMurdo Station and Scott Base as the summer average air temperatures here correlate well with Lake Hoare. The TI-model could also be applied to the other dry valleys, Wright and Victoria.

REFERENCES

Bates, D.M., and D.G. Watts, 1988. Nonlinear regression analysis and its applications. Wiley, NY, 365p.

Bomblies, A., 1998. Climatic controls on streamflow generation from Antarctic glaciers (M.Sc. thesis, University of Colorado.)

Braithwaite, R. J., 1981. On glacier energy balance, ablation, and air temperature. *J. Glaciol.*, **27**(97), 381-391.

Braithwaite, R. J., 1995. Positive degree-day factors for ablation on the Greenland ice sheet studied by energy-balance modeling. *J. Glaciol.*, 41(137), 153-160.

Chinn, T. J. H., 1987. Accelerated ablation at a glacier ice-cliff margin, Dry Valleys, Antarctica. *Arct. Alp. Res.*, **19**(1), 71-80.

Chinn, T.J., 1990. In: The dry valleys in Antarctica: the Ross Sea Region. Department of Scientific and Industrial Research, Wellington, NZ, pp. 137-153.

Clow, G.D., C. P. McKay, G. M. Simmons and R. A. Wharton, 1988. Climatological observations and predicted sublimation rates at Lake Hoare Antarctica. *J. Climatol.*, **1**(7), 715-728.

Dana, G. L., R. E. Davis, A. G. Fountain, and R. A. Wharton, Jr., 2002. Satellite-derived indices of stream discharge in Taylor Valley, Antarctica. *Hydrol. Proc.,* **16**, 1603-1616.

Doran, P. T., C. P. McKay, G. D. Clow, D. L. Gayle, A. G. Fountain, T. Nylen and B. L. Lyons. 2002, Valley floor climate observation from the McMurdo dry valleys, Antarctica, 1986-2000. *J. Geophys. Res.,* **107**(D24), 4772, doi:10.1029/2001JD002045.

Fountain, A. G., B. H. Vaughn, and G. L. Dana, 1994. McMurdo LTER: Glacier mass balances of Taylor Valley, Antarctica. *Antarctic Journal—Review,* 226-228.

Fountain, A. G., B. W. Lyons, M. B. Burkins, G. L. Dana, P. T. Doran, K. J. Lewis, D. M. McKnight, D. L. Moorhead, A. N. Parsons, J. C. Priscu, D. H. Wall, R. A. Wharton Jr and R. A. Virginia, 1999a. Physical controls on the Taylor Valley ecosystem, Antarctica: *BioScience*, **49**(12), 961-971.

Fountain, A. G., K. J. Lewis and P. T. Doran, 1999b. Spatial climatic variation and its control on glacier equilibrium line altitude in Taylor Valley, Antarctica. *Glob. Planet Change*, **22** 1-10.

Fountain, A. G., M. Tranter, T. H. Nylen, D. Booth, and K. J. Lewis, 2004. Cryconite holes on polar galciers and their importance for meltwater runoff., Antarctica. *J. Glaciol.,* **50**(168), 25-45.

Fountain, A. G., T. Neuman, P. Glenn, T. Chinn, accepted. Can warming induce advances of polar glaciers, Taylor Valley, Antarctica. *J. Glaciol*.

Fröhlich, C., 1993, Changes of total solar irradiance. *Geophysical Monograph* **75**(IUGG 15), 123-129.

Gooseff, M. N., D. M. McKnight, R. L. Runkel and B. H. Vaughn, 2003. Determining long time-scale hyporheic zone flow paths in Antarctic streams. *Hydrol. Proc*. **17** 1691-1710.

Hock, R., 1999. A distributed temperature index ice and snow melt model including potential direct solar radiation. *J. Glaciol.,* **45**(149), 101-111.

Hock, R., 2003. Temperature index melt modelling in mountain area. *J Hydrol*. **282**(1-4), 104-115.

Iqbal, M., 1983. An introduction to solar radiation. Academic Press, NY, 390p.

Jaros, C. L., 2003. Temperature-elevation effect on glacial meltwater generation in dry valley streams, Antarctica. (M. Sc. Thesis, University of Colorado.)

Johnston, R., 2004. Channel morphology and energy balance on Taylor Glacier, Taylor Valley, Antarctica. (M.Sc. thesis, Portland State University)

Kane, D. L. and R. E. Gieck, 1997. Snowmelt modeling at small Alaskan Arctic watershed. *J. Hydrol. Engineering*, **2**(4), 240-210.

Kustas, W. P. and A. Rango, 1994. A simple energy budget algorithm for the snowmelt runoff model. *Water Resour. Res*. **30**(5), 1515-1527.

Leonard, K.C., and A.G. Fountain, 2003. Map-based methods for estimating glacier equilibrium-line altitudes. *J. Glaciol.,* **49** (166), 329-336.

Lewis, K. J., A. G. G. L. Fountain and G. L. Dana, 1998. Surface energy balance and meltwater production for a dry valley glacier, Taylor Valley, Antarctica. *Ann. Glaciol*., **27,** 603-609.

Lewis, K.J., A.G. Fountain and D.L., Gayle, 1999. How important is terminus cliff melt?: a study of the Canada Glacier terminus, Taylor Valley, Antarctica. *Glob. Planet. Change*, **22**, 105-115.

McClave, J.T., and T. Sincich, 2000. Statistics, 8th Edition. Prentice-Hall, Inc., NJ, 848 p.

McKnight, D., H. House, and P. VonGuerard, 1994. McMurdo LTER: Streamflow measurements in Taylor Valley. *Antarctic Journal—Review*, 230-232.

McKnight, D. M., Niyogi, D. K., Alger, A. S., Bomblies, A., Conovitz, P. A., and Tate, C. M., 1999. Dry valley streams in Antarctica: ecosystems waiting for water. *BioScience*, **49**(12), 985-995.

Nylen, T. H. and A. G. Fountain, 2004. Climatology of katabatic winds in the McMurdo Dry Valleys, southern Victoria Land, Antarctica. *J. Geophys. Res*., **109**(D03114), doi:10.1029/2003JD003937.

Ohmura, A., M. Wild, and L. Bengtsson, 1996. A possible change in mass balance of Greenland and Antarctic Ice Sheets in the coming century. *J. Climate,* **9**, 2124-2135.

Ohmura, A., 2001. Physical basis for the temperature-based melt-index method. *J. Appl. Meteorol.* **40**, 753-761.

Paterson, W.S.B., 1994. The physics of glaciers, 3rd Edition. Pergamon, NY, 480p.